applied sciences

MDPI

Article

Therapeutic Potential of Myrrh, a Natural Resin, in Health Management through Modulation of Oxidative Stress, Inflammation, and Advanced Glycation End Products Formation Using *In Vitro* and *In Silico* Analysis

Arshad Husain Rahmani [1,*], Shehwaz Anwar [1], Ravindra Raut [2], Ahmad Almatroudi [1], Ali Yousif Babiker [1], Amjad Ali Khan [3], Mohammed A. Alsahli [1] and Saleh A. Almatroodi [1]

[1] Department of Medical Laboratories, College of Applied Medical Sciences, Qassim University, Buraydah 52571, Saudi Arabia
[2] Department of Biotechnology, National Institute of Technology Durgapur, Durgapur 713209, India
[3] Department of Basic Health Science, College of Applied Medical Sciences, Qassim University, Buraydah 52571, Saudi Arabia
* Correspondence: ah.rahmani@qu.edu.sa

Abstract: Oxidative stress, hyper-inflammatory responses, and protein glycation are the chief contributing factors in the pathogenesis of several diseases. This study aimed to explore the therapeutic role of myrrh in health management through in vitro and in silico studies. Antioxidant potential, anti-inflammatory potential, antiglycation, and advanced glycation end products (AGEs) formation inhibition activities were determined by various in vitro assays. Molecular docking was performed to predict the non-covalent binding of macromolecules (receptor) and a small molecule (ligand). Myrrh extract contained significant antioxidant activity as reflected by FRAP value (16.12 µg ascorbic acid/100 mg dry weight), the maximum percentage of DPPH scavenging (57.71%), and maximum hydrogen peroxide reducing activity (58.71%) at a concentration of 600 µg/mL. Further, the extract exhibited maximum protection from bovine serum albumin (BSA) denaturation inhibition (53.47%), anti-proteinase action (43.517%), and egg albumin denaturation inhibition (44.95%) at a dose of 600 µg/mL concentration. Myrrh is used in pharmacy as an antiseptic, anti-inflammatory, antimicrobial, antifungal, and anti-venom remedy. This study aimed to explore the antioxidant, anti-inflammatory, antiarthritic, antiglycation, and advanced glycation end products (AGEs) formation inhibition ability of methanolic myrrh extract. It was found that myrrh has good antioxidant potential due to plenty of flavonoids and polyphenolic compounds, as reflected by results of the 2,2′-diphenyl-1-picrylhydrazyl radical (DPPH) assay, FRAP (ferric reducing antioxidant power) test, and hydrogen peroxide reducing test. Furthermore, myrrh methanolic extract was found to be significantly effective against heat-induced albumin denaturation, and percent inhibition of denaturation increases with increased extract concentration. The presence of myrrh extract at a dose of 600 µg/mL decreased browning intensity (59.38%), percent aggregation index (59.88%), and percentage amyloid structure (56.13%). We used molecular docking tools to study the role of myrrh in oxidative stress (Catalase), antioxidant property (Superoxide dismutase), and antiviral property (spike protein S). The molecular docking analysis confirmed four phytoconstituents; 2,3-Furandione, Curzerene, delta-Elemene, and Furanoeudesma-1,3-Diene interact with catalase and superoxide dismutase. Curzerene and Furanoeudesma-1,3-Diene showed remarkable interaction with SARS-CoV-2 spike protein S. Our data suggest that myrrh resin extract can be used to develop a suitable alternative therapy for various diseases linked with oxidative stress, inflammation, glycation, and AGEs.

Keywords: myrrh; reactive oxygen species (ROS); oxidative stress; anti-inflammatory activity; anti-glycating property

Citation: Rahmani, A.H.; Anwar, S.; Raut, R.; Almatroudi, A.; Babiker, A.Y.; Khan, A.A.; Alsahli, M.A.; Almatroodi, S.A. Therapeutic Potential of Myrrh, a Natural Resin, in Health Management through Modulation of Oxidative Stress, Inflammation, and Advanced Glycation End Products Formation Using *In Vitro* and *In Silico* Analysis. *Appl. Sci.* **2022**, *12*, 9175. https://doi.org/10.3390/app12189175

Academic Editors: Antony C. Calokerinos and Wojciech Kolanowski

Received: 30 July 2022
Accepted: 9 September 2022
Published: 13 September 2022

1. Introduction

The roles of oxidative stress and reactive oxygen species (ROS) in the development of neurological disorders, cancer, and diabetes have been well established. Oxidative stress is an imbalance when the body's oxidizing systems, which include numerous free radicals such as reactive oxygen species (ROS) and reactive nitrogen species (RNS), as well as antioxidant systems, which counteract those potentially dangerous free radicals, are out of equilibrium. Oxidative stress has been further reported to be linked with infections, notably those caused by RNA viruses that include corona viruses [1]. Diabetes mellitus is a chronic disease indicated by an unusually high blood glucose level, technically known as hyperglycemia [2]. Diabetes mellitus type 2 has already been known to be a risk factor for SARS-CoV-2 infection. It is reasonable to speculate that hyperglycemia may have a role in the glycation of this protein, triggering a chain of events that results in acute respiratory distress syndrome and mortality of patients with COVID-19 [3].

Protein glycation changes protein molecular structure, altering enzyme or receptor functioning and activity, and hence plays a vital role in the development of illnesses. Under hyperglycemic conditions, advanced glycation end products (AGEs) have been found to be elevated in diabetes mellitus. It is produced by the glycation of biomolecules [2,4]. COVID-19 risk factors have been connected to AGEs [5].

AGEs create crosslinks with many biomolecules, including proteins, and interact with plasma membrane local AGE receptors (RAGE), modulating intracellular signaling, expression of genes, and the production of free radicals and pro-inflammatory chemicals [6]. AGE/RAGE signaling in diabetes-mediated vascular calcification has been reported to be linked with oxidative stress [7]. Further, the increased production and accumulation of ROS at the inflammatory sites cause tissue damage and endothelial dysfunction leading to inflammatory disorders [8]. Various events such as protein denaturation, increased vascular permeability, and pain are important for inflammation. Chronic inflammation has been found to be involved in cancer development [9]. AGE-modified proteins produce proteinase-resistant and detergent-insoluble aggregates, as well as autoantibodies [10].

A number of medicinal plants have been identified to be very beneficial in the prevention and treatment of a wide variety of diseases [11]. Myrrh resin is a transparent yellow resin from the tiny, thorny stems of the Commiphora genus tree, most often from *Commiphora myrrha* and *C. molmol* species [12]. Myrrh is commonly used as an antiseptic for wounds [13], as a pain reliever [14,15], and in the cholesterol metabolism [16]. In search of new, economic, and effective therapeutic agents against morbidity and mortality of diabetic patients, the purpose of this research is to look at the molecular and cellular effects of myrrh on AGEs' formation, glycation, inflammation, oxidative stress, and other chronic disease risk factors such as oxidative stress using in vitro and in silico studies. The purpose of molecular docking investigations involving superoxide dismutase and catalase with myrrh compounds was to explore the antioxidant activities of myrrh resin extract in reducing oxidative stress and to link the most interesting components to their chemical properties, as well as to explore possible antiviral properties.

2. Materials and Methods

2.1. Materials

Myrrh dried flakes (resin) were purchased from the local market, Qassim, Saudi Arabia. Ascorbic acid, DPPH (2,2-diphenyl-1-picrylhydrazyl), Folin-CioCalteau reagent, ferric chloride, potassium ferricyanide, trichloroacetic acid, quercetin, gallic acid, trypsin, and Congo red were obtained from Sigma Co. St. Louis, MO, USA. Other chemicals including DMSO, hydrogen peroxide (H_2O_2), Methanol, Aluminum Chloride, Hydrochloric Acid, Sodium Carbonate, Monosodium Dihydrogen Phosphate, Disodium Hydrogen Phosphate, and Sodium Hydroxide were purchased from Merck, Darmstadt, Germany.

There are different types of laboratory reagents, but only one type is suitable for all applications. There are different requirements for each strategy. In accordance with the application test in the product specification, the product was assessed for this strategy.

High purity analytical grade reagents are ideal for use in analytical applications. As a result, chemicals and reagents of the analytical grade were employed throughout the study. After removing volatile impurities using a distillation process, high purity solvents are created through filtration to make HPLC grade solvents. If these contaminants are found, they will contaminate the column and shorten its lifespan. The solvents used in this study were therefore of HPLC quality.

2.2. Experimental

2.2.1. Myrrh Methanolic Extract Preparation

The resinous plant material was acquired from a local market having a regulatory framework of vendors in Buraydah, Qassim; this framework has a more stringent control and monitoring of herbal products' quality and safety. We purchased the dried flakes by this local network after the full enquiry based on conversations, observations, and evidence in this regard. The plant material was thoroughly prewashed with water before being shed dried for three days at room temperature. After drying, the sample (50 g) was roughly crushed to make a homogeneous powder, then extracted for five days with 500 mL of methanol and occasional shaking. It was assumed that no possible myrrh components were lost during extraction. After filtration of raw extract and vacuum-drying, the dried extract was kept in the refrigerator until needed. As per the experiment requirements, the filtrate was regenerated in the required amount of water or dimethyl sulfoxide (DMSO). DMSO is a solvent commonly utilized in drug discovery. Protein denaturation, aggregation, or disintegration can occur as a result of DMSO changing the characteristics of proteins in solution. Moreover, the apparent binding characteristics of proteins can also be altered by DMSO. This might be due to the physiochemical characteristics of the molecule or protein in DMSO, DMSO interference on the analyzing technique, or a combination of the three. Therefore, the characterization of compounds and proteins in low-DMSO compatible assay buffers is critical for high-quality drug discovery. As a result, 0.1% DMSO was employed in this current study via serial dilution of several stock solutions. The extraction yield was used to compute the extract yield (%) [16].

$$\text{Extraction yield (\%)} = (w/W) \times 100$$

where w denotes the weight of dry extract (g), and W refers to the weight of sample used for extraction (g).

2.2.2. Phytochemical Screening

A previously published study was used to undertake phytochemical analysis of the extract for saponins, carbohydrates, alkaloids, flavonoids, phenolic compounds, tannins, and anthraquinone [16]. Carbohydrate identification was achieved by combining 1000 µL of iodine solution with 3000 µL of extract produced separately in methanol. If the coloration shifts to purple, the presence of carbs may be confirmed. The saponins were diagnosed in a test tube by combining 5 mL distilled water with 5 mL extract and vigorously shaking the mixture before heating the vial. The formation of steady foam indicates the presence of saponins.

Meanwhile, a vial was filled with 2.0 mL of plant extract and 2.0 mL of distilled water. The presence of condensed tannins was revealed by the development of green precipitation after adding a small amount of $FeCl_3$. When 2.0 mL of myrrh extract was mixed with sodium hydroxide (20%) solution, a bright yellow color developed, indicating the presence of flavonoids in extracts. However, when dilute HCl was added, the yellowish hue turned colorless. The development of such a blue-black color when a few drops of $FeCl_3$ were added to the extracts confirmed the phenolic compounds' existence.

2.2.3. Polyphenol Content Evaluation

The Folin-Ciocalteu reagent was used to quantify total polyphenol content (T), as reported in previous research [9]. Gallic acid (50, 75, 100, 125, 150, 200, and 250 µg/mL) was

employed as a control. The total polyphenol content of the extract was evaluated using the calibration plot, which was represented in mg Gallic Acid Equivalents (GAE). The results of the study were represented as mg Gallic acid equivalents per gram sample extract after three times test repetition.

$$T = P \times Z/M$$

where, the quantity (mL) of sample utilized in the extraction is denoted by P. The weight of the purified dry sample utilized is M, and Z is the gallic acid content in mg/mL (g).

2.2.4. Total Flavonoid Content

The total flavonoid content (F) of myrrh extract was investigated through aluminum chloride ($AlCl_3$) assay outlined in a recent publication [9]. A calibration curve was created using quercetin (20, 25, 75, 100, 150, 200, and 250 µg/mL). In a nutshell, myrrh extract (50 µg/mL; 500 µL) or quercetin solution were combined thoroughly with $AlCl_3$ (500 µL; 2%). After incubation for 1 h at room temperature and recurrent shaking, the absorbance was read at 420 nm with a spectrophotometer against methanol as blank. The total flavonoid content was explored as mg of quercetin equivalent per gram sample extract using the calibration plot.

$$F = Z \times P/M$$

where, Z is the quercetin content in mg per ml, P specifies the amount (mL) of material (sample) utilized for the extraction, and M denotes the weight of purified dry sample utilized (g).

2.2.5. Reference Drug Preparation

The reference medications, ibuprofen and diclofenac sodium, were ground into a fine powdery drug material separately. We weighed 200 mg of powdery drug materials on a digital analytical balance and combined them with double-distilled water (20 mL) to make clear solutions in separate vessels. Ibuprofen was serially diluted in phosphate buffer (pH 6.4) for the test of inhibition of heat-induced denaturation inhibition. Diclofenac sodium, on the other hand, was prepared by diluting in Tris HCl buffer, pH 7.4, for anti-proteinase activity testing [17]. Studies of active drug/excipient compatibility represent an important phase in the pre-formulation stage of the development of all dosage forms. Keeping this in mind, we had already standardized the concentration of drugs for various experiments in our previously published research articles that were not affected by the presence of any disintegrant and glidant agent.

2.2.6. Assessment of Reduction Capacity

This test was carried out with minor modifications according to the method published in previous papers [6]. At room temperature, this test assessed the ability of the myrrh extract (50, 75, 100, 200, 300, 400, 500, and 600 µg/mL) to reduce ferric ions into ferrous ions. The reaction led to a shift in absorbance measured at a wavelength of 700 nm against phosphate buffer (pH 6.6) for both the control and test samples. All of the tests were repeated three times. The formula described below was used to compute the percentage reducing capacity.

$$\text{Percentage reduction capacity} = [(Lc - Ls)/Lc] \times 100$$

where, the absorbance of the control is denoted by Lc (extract was absent) and the absorbance of extract-containing solution is indicated by Ls.

2.2.7. Hydrogen Peroxide Scavenging (H_2O_2) Activity

This activity was studied using the approach outlined by a previously published article [6]. with minor modifications. The extract or ascorbic acid (50, 75, 100, 200, 300, 400, 500, and 600 µg/mL) and 1 mL of 40 mM H_2O_2 (prepared in phosphate buffer, pH 7.4) were mixed in different vials. Following 10 min of incubation, the absorbance of all solution was evaluated at 230 nm against phosphate buffer. All of experiments were performed in

triplicate in total. By using the equation provided beneath, the percent scavenging capacity of myrrh extract was estimated.

$$\text{Reduction capacity (\%)} = [(Lc - Ls)/Lc] \times 100$$

where, the absorbance of the control is denoted by Lc (H_2O_2 solution only) and the absorbance of H_2O_2 solution containing extract is indicated by Ls.

2.2.8. DPPH Assay

This capacity of myrrh was conducted utilizing a test involving DPPH (1,1 diphenyl-2-picryl-hydrazyl) radical according to our previously published article [17]. Myrrh extract (50, 75, 100, 200, 300, 400, 500, and 600 µg/mL) and 1 mL of 0.3 mM methanolic DPPH solution were mixed in different vials, and solutions were placed in a dark place for 30 min. The absorbance was noted at a wavelength of 517 nm against methanol. Only the DPPH solution which was prepared in methanol was present in control.

$$\text{Percent DPPH scavenging potential} = [(Lc - Ls)/Lc] \times 100$$

where, the absorbance of the control is denoted by Lc (DPPH in methanol, and the extract was absent) and the absorbance of the DPPH solution with the extract is indicated by Ls.

2.2.9. Inhibition Potential of Myrrh Extract against Heat Induced Albumin Denaturation

The possible anti-inflammatory capacity of Myrrh extract can be assessed by the albumin denaturation inhibition method as described by previous researchers [17,18] using ibuprofen as a reference anti-inflammatory drug. An amount of 1 mL of 1% BSA (bovine serum albumin) was mixed with equal volume of either myrrh extract (50, 75, 100, 200, 300, 400, 500, and 600 µg/mL) or ibuprofen (100 and 200 µg/mL). The setups were incubated at room temperature over 20 min. These reaction sets then were processed over 30 min to 71°C in a water bath to promote BSA denaturation. The solutions were cooled down, and optical density of individual setups was noted at a wavelength of 660 nm using blank having distilled water only. The negative control had 1 mL phosphate buffer (pH 7.4) and 1.5 mL of 1% BSA.

$$\text{Inhibition of BSA denaturation induced by heat (\%)} = [(Lc - Ls)/Lc] \times 100$$

where, the optical density of the control, i.e., the test solution without extract or ibuprofen, is Lc; the optical density of the test solution with extract or ibuprofen is Ls.

2.2.10. Test for Proteinase Action Inhibition

Proteinases are found in lysosomes and are known to catalyze the hydrolysis of proteins. It has been reported that leukocyte proteinases contribute to tissue damage in inflammatory reactions and proteinase inhibitors offer protection against proteinase-induced tissue damage [19]. Proteinase enzyme inhibitory activity of myrrh extract was investigated according to our previously published articles [20] using diclofenac sodium (200 µg/mL) as a reference drug. Various aliquots of myrrh extract (50, 75, 100, 200, 300, 400, 500, and 600 µg/mL) were used for this assay. The optical densities of various samples were recorded at a wavelength of 210 nm against blank having Tris HCl buffer only. The negative control setup was made up of 1 mL normal saline (0.9 % NaCl), 1 mL Tris HCl buffer, 0.06 mL trypsin, 1 mL 0.8 percent casein, and 2 mL 70% perchloric acid.

$$\text{Inhibition of proteinase action (\%)} = [(Lc - Ls)/Lc] \times 100$$

where, the absorbance of the control, i.e., the test solution without extract or diclofenic, is Lc; the absorbance of the test solution with extract or diclofenac is Ls.

2.2.11. Egg Albumin Denaturation Inhibition for Anti-Arthritic Activity

An amount of 2.8 mL of fresh phosphate buffer saline (pH 6.4), 0.2 mL of chicken egg albumin, and 2 mL of either diclofenac sodium (200 µg/mL) or myrrh extract (50, 75, 100, 200, 300, 400, 500, and 600 µg/mL) were placed at room temperature for 15 min inside an incubator [17,21]. Following the incubation, various test solutions were later put at 70 °C for 5 min. At 660 nm, the absorbance of all solutions was measured against phosphate buffer as a blank.

$$\text{Inhibition of egg albumin denaturation (\%)} = [(Lc - Ls)/Lc] \times 100$$

where, the absorbance of the control, i.e., the test solution without extract or diclofenac, is Lc; the absorbance of the test solution with extract or diclofenac is Ls.

2.2.12. Screening for Antiglycation Property of Myrrh Extracts

a. Incubation of Myrrh extracts with in vitro glycation system

The Brownlee approach was used to perform the in vitro glycation of BSA [22]. BSA (10 mg/mL) and glucose (500 mM) were put in sterilized tubes together with varied amounts of myrrh extract (50, 75, 100, 200, 300, 400, 500, and 600 g/mL), either with or without a 0.1 M phosphate buffer (pH 7.4). The tubes were kept in the dark at 37 °C for 15 days. Glass vials that had been autoclaved, closed, and capped were used to ensure sterility. After incubation, the samples underwent overnight phosphate buffer dialysis at room temperature to remove bound and unbound glucose. The concentration of BSA was determined using the molar extinction coefficient method. After that, the samples were kept at −20 °C until testing could be performed on them. The experiments were all carried out in triplicate.

b. Effect of Myrrh extracts on browning in glycated samples

Glycation is assumed to play a major role in the development of diabetes and its consequences [2]. The degree of browning in glycated samples is said to be an effective indicator of glycation in many samples [9]. After diluting with distilled water, the browning intensity was evaluated by monitoring the absorbance of various glycated samples at 420 nm [22] that used a 1 cm path length cell. All of the tests were performed in triplicate. The following formula [9] was used to calculate the relative percentage browning intensity.

$$\text{Percentage protection} = [(Lc - Ls)/Lc] \times 100$$

where, Lc refers to absorbance of BSA and glucose system (without extract). However, Ls denote absorbance of BSA and the glucose system (with extract).

c. Effect of Myrrh extract on protein aggregation index

The aggregation index is a semi-quantitative measure of the level of aggregation in protein samples such as antibodies that may be evaluated by evaluating the material's UV/Visible spectrum (https://resources.perkinelmer.com/lab-solutions/resources/docs/ABR-Determination-of-MonoclonalAntoibodyAggregationUsing-UV-Vis-Spectrosocpy.pdf accessed on 1 January 2020).

The aggregation index is considered to be an indicator of relative aggregation [23].

The absorbance of several glycated samples with (50, 75, 100, 200, 300, 400, 500, and 600 µg/mL) and without extract was measured at 280 and 340 nm to determine the protective capacity of myrrh extract against aggregation by quantifying the percentage of protein aggregation index.

$$\text{Percentage of protein aggregation index} = [L_{340}/(L_{280} - L_{340})] \times 100$$

where, L_{340} = Absorbance of the glycated sample at 340 nm and L_{280} = Absorbance of the glycated sample at 280 nm.

d. Determination of fibrillar state by Congo red assay

The Congo red investigation was performed to determine how much glycation-induced fibrillation of BSA was inhibited. Glycation-induced fibril formation in various BSA samples was determined on the basis of interaction of amyloid-specific dye Congo red (CR). Congo red (an amyloid-specific dye) was produced as described in earlier studies. The absorbance was measured individually for AGEs-BSA having myrrh extract (50, 75, 100, 200, 300, 400, 500, and 600 µg/mL), AGEs-BSA alone, native BSA, as well as for the Congo red background. In a nutshell, 500 µL of AGEs-BSA/native BSA (100 µM) and 100 µL of Congo red (100 µM) were placed for 10 min at 37 °C. Each sample's absorbance was measured at 530 nm.

$$\text{Percent prevention of amyloid formation} = [(Lc - Ls)/Lc] \times 100$$

where, Lc stands for BSA and glucose system absorbance (without extract) and Ls for BSA and glucose system absorbance (with extract).

2.2.13. Biophysical Investigations

A stock of BSA (1 mg/mL) was created using sodium phosphate buffer (20 mM, pH 7.4). In order to encourage glycation, BSA (0.2 mg/mL) and glucose (0.5 M) were kept together in sterilized tubes with 20 mM sodium phosphate buffer (pH 7.4). These tubes were then placed in a water bath shaker at 37 °C for 15 days. The reference or control sample, BSA, was incubated by itself with phosphate buffer (20 mM, pH 7.4). The application of sodium azide (3 mM) prevented bacterial infection. After incubation, sodium phosphate buffer was used to dialyze the solutions at 4 °C (0.1 M, pH 7.4).

The presence of 50, 75, 100, 200, 300, 400, 500, and 600 g/mL of myrrh extract was used to treat BSA (0.2 mg/mL) with glucose (0.5 M) in 20 mM sodium phosphate buffer (pH 7.4) in autoclaved tubes to test if it might prevent glycation and AGE development. Biophysical techniques like UV absorption, AGEs-specific fluorescence, and ThT fluorescence were utilized to assess the defense against glycation and the production of AGEs.

a. UV Absorption

Utilizing a dual beam Perkin Elmer Lambda 25 spectrophotometer, UV absorption experiments were carried out. The UV spectra of BSA (0.2 mg/mL) were examined in the presence or absence of glucose and myrrh extract over the wavelength range of 240–500 nm. Each sample's absorbance intensity was measured at 280 nm [24–26].

b. AGEs-specific fluorescence study

All measurements of fluorescence were performed using a Shimadzu spectrofluorometer, model RF-5301PC. However, protection against the production of luminous AGE products was examined with excitation at 350 nm and emission in the range 400–480 nm. The slit widths for excitation and emission were 3 nm [26].

c. Thioflavin T-specific fluorescence study

Every sample had 6 µM Thioflavin T added to it to show the extract's fibrillar state inhibitory properties. Fluorescence spectra of each sample were obtained at 440 nm for excitation and 450–600 nm for emission. The slit widths for excitation and emission were 10 nm [24].

2.2.14. Statistical Analysis

The research was conducted in three separate studies, and the results were presented as mean standard error. ANOVA was employed for statistical analysis after data entry.

2.2.15. Docking Studies

Molecular docking is the *in-silico* modeling of two or more molecules to create a stable product. Docking depicts the three-dimensional structure of any complex based on the

properties of target molecules, such as protein or DNA and ligand [27]. The program's score function rates and classifies various possible adduct structures made via molecular docking. The best-docked conformers are suggested via docking simulations based on the system's total energy. The ultimate objective is to predict bound conformations and binding affinity [28].

a. The Receptors

The SARS-CoV-2 spike glycoprotein was chosen to test the antiviral properties of myrrh, and the catalase and superoxide dismutase (SOD) enzymes were chosen for molecular docking research to predict the interaction of metabolites of the myrrh resin extract with two major enzymes of the cellular anti-oxidant mechanism.

The three-dimensional structures of human erythrocyte catalase 3-amino-1,2,4-triazole complex (PDB id: 1DGH) [29] and human SOD1 complexed with iso-proteranol (PDB id: 5YTU) [30] and the SARS-CoV-2 spike glycoprotein (closed state) (PDB id: 6VXX) [31] were downloaded from Protein Databank (https://www.rcsb.org/, accessed on 23 January 2022). The structures were chosen based on resolution, source organism, and availability of the bound ligand for active site reference. Receptor crystal structures were discovered using X-ray diffraction at wavelengths of 2, 1.9, and 2.8 nm, respectively.

b. The Ligands

The active constituents of myrrh resin are 2,3-furandione, Curzerene, delta-Elemene, and Furanoeudesma-1,3-Diene [32]. All of the ligands' three-dimensional structures were retrieved in structure-data file (SDF) format from the NCBI PubChem compounds database (https://pubchem.ncbi.nlm.nih.gov, accessed on 23 January 2022) [33]. Then, using the Open Babel program (https://sourceforge.net/projects/openbabel/, accessed on 23 January 2022), these files were translated into the Protein Databank (PDB) file format. Tables 2 and 3 provide comprehensive details on the ligands and their properties.

c. Molecular Docking

A sophisticated computational modeling method for figuring out how a ligand (phytochemicals or other substances) interacts with the active site of an enzyme or receptor is called molecular docking. Through the use of molecular docking, the interaction between the substrate and enzyme was identified. The proteins were processed appropriately in Biovia Discovery Studio Visualizer (https://discover.3ds.com/discovery-studio-visualizer-download/, accessed on 23 January 2022) and docked using AutoDock vina (https://vina.scripps.edu/, accessed on 23 January 2022).

Before docking, the hydrogen atoms were added, charges were applied, all crystallographic water molecules were eliminated, and default values for other parameters were selected. For 1DGH along the size 20 for the X-, Y-, and Z-axis, the docking grid dimensions were center x = 25.0, center y = 40.0, center z = 60.0, and for 5YTU along the size 20 for X-, Y-, and Z-axis, the docking grid dimensions were center x = −67.09, center y = 32.2, center z = 20.5. While the X-, Y-, and Z-axis along the size 20 of the grid for 6VXX of the docking were center x = 181.11, center y = 233.11, and center z = 243.26.

Before the docking experiment, polar hydrogens were given to each protein receptor, and Kollman's partial atomic charges were employed to lower the energy. The processed receptor structure was stored in the AutoDock PDBQT file format, which includes hydrogens in all polar residues (Protein Data Bank, Partial Charge (Q), and Atom Type (T)). The receptor and ligands were processed by adding hydrogen atoms using the software MGLtools Version 1.5.7 (https://ccsb.scripps.edu/mgltools/downloads/, accessed on 23 January 2022) [34]. The most runs possible were limited to 8. The best docking in terms of binding free energy (expressed as negative values) was assessed for the following investigation.

d. Validation of Docking Study

The binding of molecules in the enzyme's active site can happen at random. So, using positive, we conducted a controlled investigation to verify the prior docking. Since

research teams already examine 1DGH, 5YTU, and 6VXX, NADPH (Dihydronicotinamide-Adenine Dinucleotide Phosphate) [PubChem CID 5884], Levisoprenaline [PubChem CID 443372], and Acetylglucosamine [PubChem CID 24139] are employed as positive controls for these molecules [29–31]. Using AutoDock Tools and AutoDock Vina, a docking study for a positive control was carried out, with the Grid box adjusted so that all the control compounds could bind at the same pocket where they are intended to bind. The coordinate values for the corresponding testing chemicals were maintained. The other variables remained the same. The water molecules were eliminated before the docking analysis.

3. Results

Our most recent in vitro research indicates that myrrh extract has excellent antioxidant properties, anti-inflammatory properties, and it has good protection ability against heat-induced albumin and egg albumin denaturation. Additionally, the myrrh extract inhibits the formation of cross-amyloid and AGEs, stops the glucose-mediated browning of BSA, and has antifungal and antibacterial properties. The interaction between functional residues of the SARS-CoV-2 virus' spike protein and myrrh phytocontents has been confirmed by molecular docking analysis. Since the molecules found in myrrh extract have been found to be potential inhibitors of the SARS-CoV-2 spike protein using molecular docking, myrrh consumption may be advantageous against COVID-19 as well as in the prevention and treatment of complications related to COVID-19.

3.1. Preliminary Observations, Flavonoid, and Phenolic Content

The preliminary observations of myrrh extract show that 50 g of dry resin powder gives a 3.18% yield. Its methanol extract had reddish brown color and sticky texture, and it did not contain any specific odor. The results of phytochemical screening of myrrh resin extract for the presence of various phytoconstituents are provided in Table 1. Total polyphenolic compounds (T) in methanolic extracts of myrrh was 19.54 ± 0.016 mg GAE per g dry weight of the extract. The rounding of quantities of polyphenolic content and flavonoid contents were carried according to guidelines as published by NIST. For general number rounding conventions and conversion factors for quantities expressed in a variety of units, the general rules were followed as provided by a previously published article (https://www.nist.gov/pml/special-publication-811/nist-guide-si-appendix-b-conversion-factors, accessed on 23 January 2022). A reasonable quantity of flavonoids was found in myrrh extract and was 11.58 ± 0.01 mg QUE/g dried weight of extract, but the amount of flavonoids was lower than the phenolic content.

Table 1. Phytochemical screening of myrrh.

Phytochemical Constituents	Resin
Alkaloids	+
Saponins	-
Tannins	+
Flavonoids	+
Glycosides	+
Terpenoids	+
Phenolic compounds	+

3.2. H_2O_2 Reducing Ability

A high level of H_2O_2 scavenging activity of myrrh extract has been noticed, and this H_2O_2 scavenging ability was shown to increase with an increase in the quantity of extract (Figure 1). Therefore, myrrh extract might have a significant ability to reduce hydroxyl free radicals formed by breakdown of H_2O_2, and the activation of neutrophils in the blood contributing to the prevention of oxidative stress. H_2O_2 reduction by different concen-

trations of myrrh may be attributed to the electron-donating potential of polyphenolic bio-active molecules of myrrh extract. This activity of myrrh is very significant because the dissociation of H_2O_2 leads to the hydroxyl radical formation.

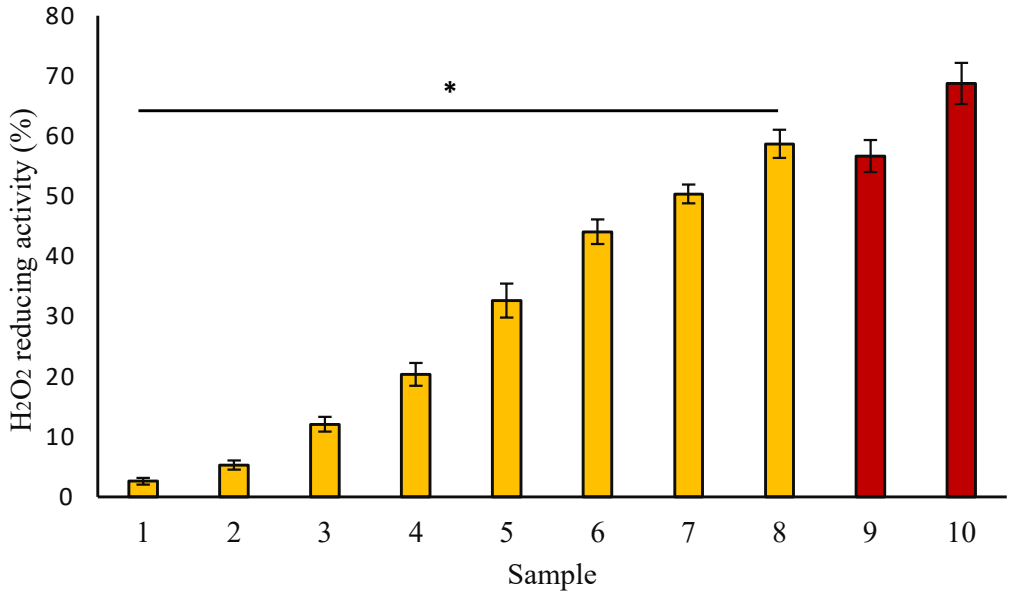

Figure 1. H_2O_2 reducing ability (%) of myrrh methanolic extract. Samples 1 to 8 (yellow bar) correspond to various concentrations of extract (50, 75, 100, 200, 300, 400, 500, and 600 µg/mL). Samples 9 and 10 (red bar) correspond to samples having 100 and 200 µg/mL concentrations of ascorbic acid. The data are shown as means ± standard error of the means (n = 3, $p < 0.05$). The statistical differences are represented with an asterisk (*) for myrrh denoting significance at $p < 0.05$ in comparison with the reference sample.

3.3. Reducing Power Estimation by FRAP Assay

Ascorbic acid was utilized as a control, and ascorbic acid solution (50–250 µg/mL) obeyed Beer's Law at a particular wavelength of 700 nm with R^2 (regression co-efficient) of 0.9965. The slope (m) of the plot was 0.0027, while the intercept was 0.0226. The standard equation of the curve was Y = 0.0027x + 0.022. The FRAP value of myrrh extract was calculated to be 16.12 ± 0.058 µg ascorbic acid/100 mg dry weight of extract. In terms of absorbance, the reducing power of myrrh extract was observed to be proportionately enhanced in a concentration-dependent way. The FRAP value of myrrh extract was 0.72 ± 0.31 mM $FeSO_4$/g extract. Presentation of results and simple linear regression analysis were carried out according to IUPAC Recommendations, 1994 (Currie and Svehla, 1994).

3.4. DPPH Assay

The reduction of the DPPH free radical is used to determine the free radical scavenging potentials of antioxidant substances. The data of the DPPH assay of myrrh extract are presented in Figure 2. The data shows that myrrh extract has a meaningful ability to reduce the DPPH free radical, and the reduction of DPPH becomes increased with an increase in myrrh extract ($p < 0.05$).

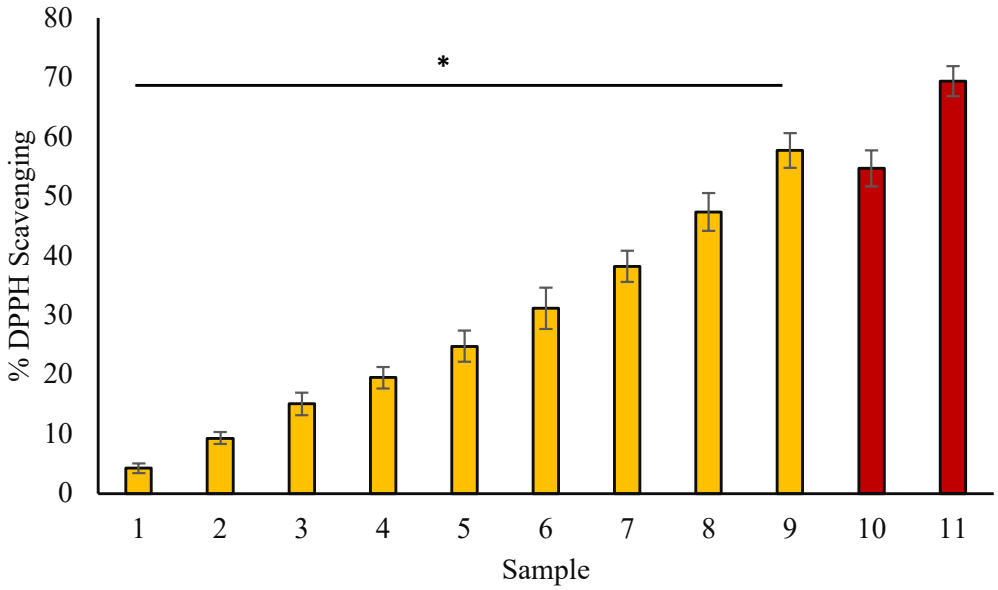

Figure 2. Percent of DPPH scavenged vs. concentration (µg/mL). Samples 1 to 9 (yellow bar) correspond to various concentrations of extract (50, 75, 100, 150, 200, 300, 400, 500, and 600 µg/mL). Samples 10 and 11 (red bar) correspond to samples having 100 and 200 µg/mL concentrations of ascorbic acid. The data are shown as means ± standard error of the means (n = 3, $p < 0.05$). The statistical differences are represented with an asterisk (*) for myrrh denoting significance at $p < 0.05$ in comparison with the reference sample.

3.5. Albumin Denaturation Inhibition

Our data showed concentration-dependent inhibition of heat-mediated BSA denaturation, and protection towards denaturation becomes increased with an increase in the myrrh quantity in samples (Figure 3) ($p < 0.05$). At a concentration of 200 µg/mL, ibuprofen demonstrated the greatest inhibition (57.15%).

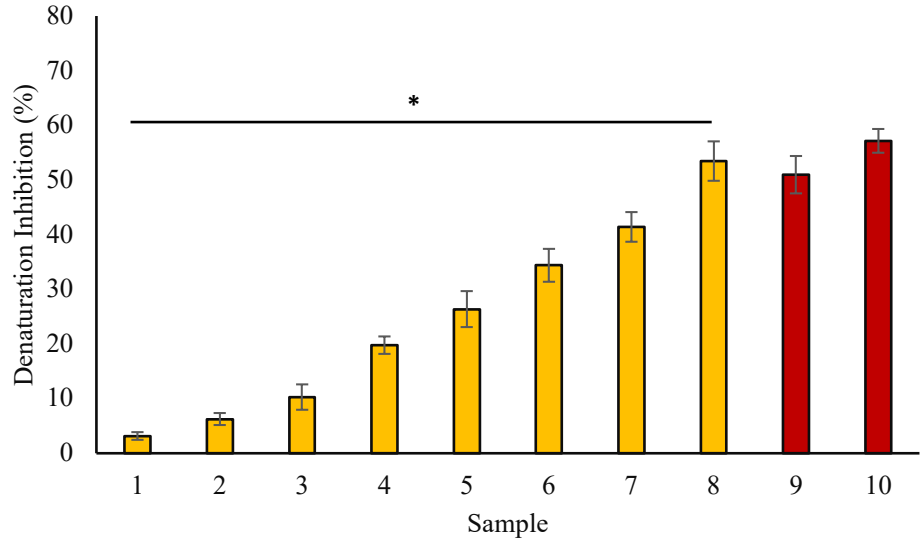

Figure 3. Percentage inhibition of heat-induced denaturation of albumin. Samples 1 to 8 (yellow bar) correspond to various concentrations of extract (50, 75, 100, 200, 300, 400, 500, and 600 µg/mL). Samples 9 and 10 (red bar) correspond to 100 and 200 µg/mL concentrations of ibuprofen. The data are shown as means ± standard error of the means (n = 3, $p < 0.05$). The statistical differences are represented with an asterisk (*) for myrrh denoting significance at $p < 0.05$ in comparison with the reference sample.

3.6. Inhibition of Proteinase Action

Methanolic extracts of myrrh exhibited significant proteinase inhibitory capacity, and this potential of myrrh was found to increase with an increase in the quantity of myrrh extract. Myrrh extract showed highest inhibition activity (43.517%) at a concentration of 600 µg/mL (Figure 4) ($p < 0.05$). However, diclofenac sodium showed a maximum inhibition of 57.91% at 200 µg/mL.

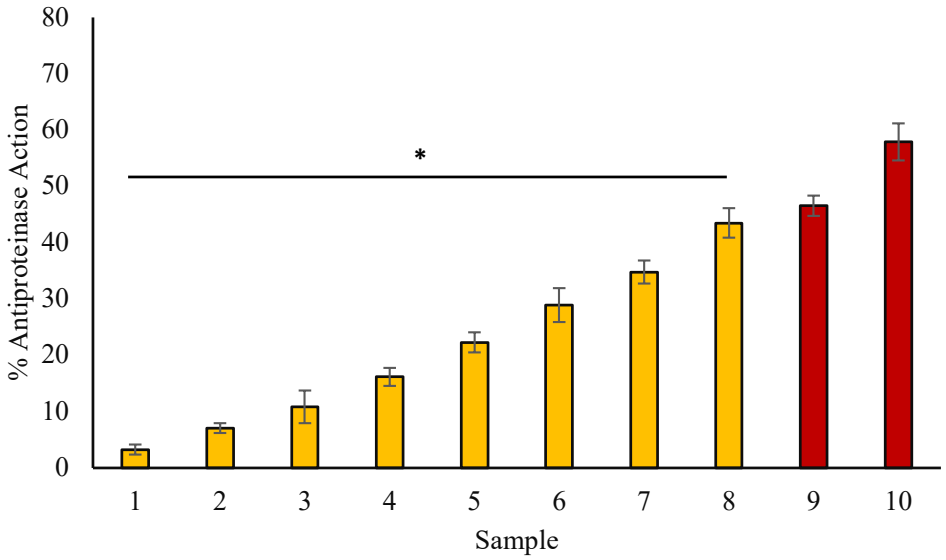

Figure 4. The percentage inhibition of proteinase action. Yellow columns (1–8) represent samples with various concentrations (50, 75, 100, 200, 300, 400, 500, and 600 µg/mL) of myrrh extract. The red columns (9 and 10) represent samples having 100 and 200 µg/mL concentrations of diclofenac, respectively. The data are shown as means ± standard error of the means (n = 3, $p < 0.05$). The statistical differences are represented with an asterisk (*) for myrrh denoting significance at $p < 0.05$ in comparison with the reference sample.

3.7. Inhibition of Egg Albumin Denaturation

The possible anti-arthritic potential of myrrh extract was tested towards egg albumin denaturation (Figure 5). Egg albumin denaturation significantly decreased by plant extract in a concentration-dependent approach (50, 75, 100, 200, 300, 400, 500, and 600 g/mL). Our findings demonstrate that a myrrh extract is very efficient in preventing heat-induced denaturation of egg albumin, and that the percent inhibition of denaturation increases as the extract concentration increases ($p < 0.05$). At a concentration of 200 µg/mL, diclofenac demonstrated the highest inhibition of 59.67% in the current study.

3.8. Effect of Myrrh Extract on Browning Intensity in Glycated Samples

The samples having BSA and glucose with a range of myrrh extract concentrations showed significantly reduced browning intensity as compared with samples having BSA and glucose. The methanolic extract of myrrh extract exhibited 59.387% at 600 µg/mL browning in comparison with BSA that was kept with glucose (without extract) (Figure 6) ($p < 0.05$). The data confirm that the extract inhibited the formation of glycated brown products.

3.9. Effect of Myrrh Extract on Protein Aggregation Index

The results of the study showed that myrrh extract significantly reduced protein aggregation. BSA samples having glucose and myrrh extract showed a very significant decrease in aggregation index in comparison with BSA incubated with glucose alone in a concentration-dependent manner (Figure 7) ($p < 0.05$).

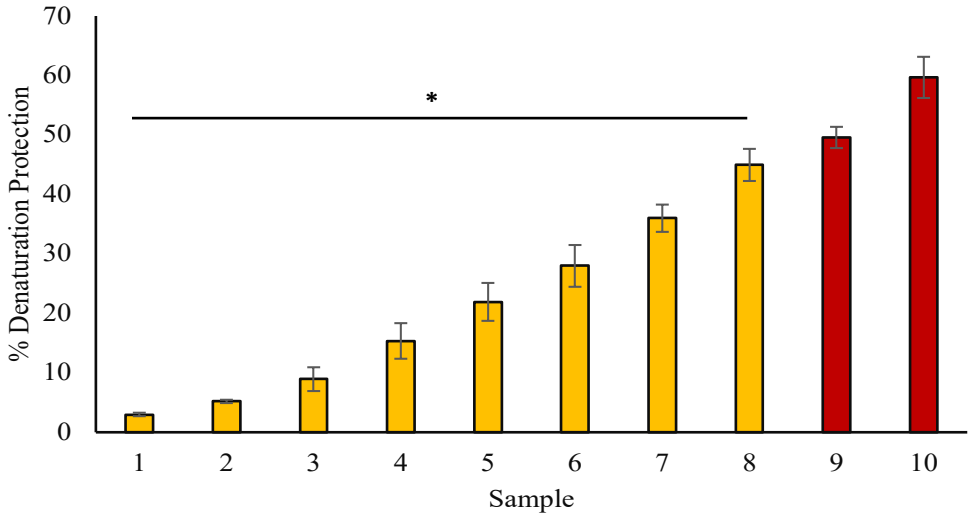

Figure 5. Egg albumin denaturation protection (%). Yellow columns (1–8) represent samples with various concentrations (50, 75, 100, 200, 300, 400, 500, and 600 µg/mL) of myrrh extract. The red columns (9 and 10) represent samples having 100 and 200 µg/mL concentrations of diclofenac, respectively. The data are shown as means ± standard error of the means (n = 3, $p < 0.05$). The statistical differences are represented with an asterisk (*) for myrrh denoting significance at $p < 0.05$ in comparison with the reference sample.

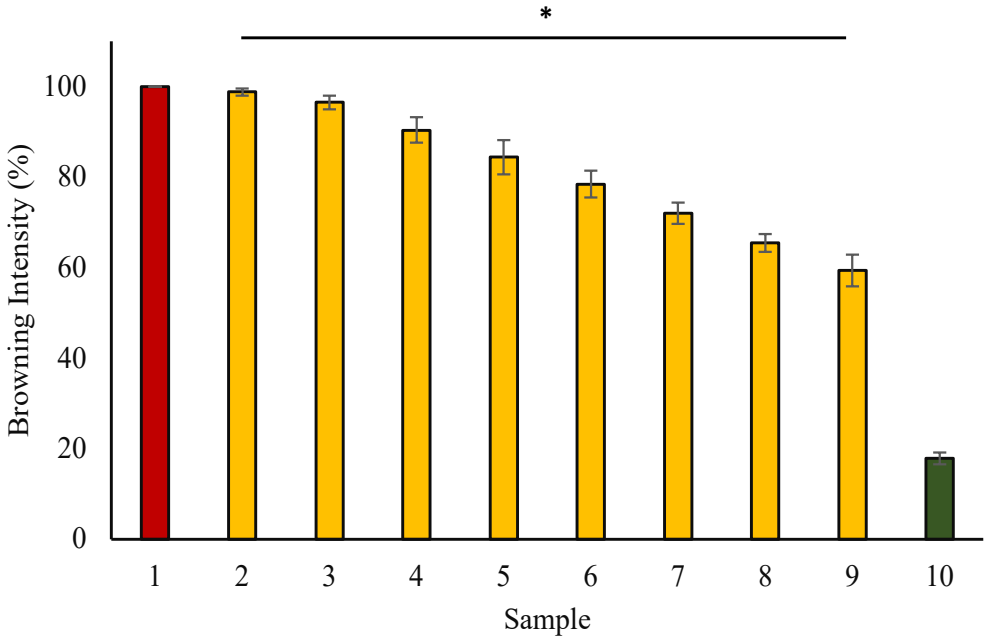

Figure 6. Decrease in browning in presence of myrrh. Sample 1 denotes BSA having glucose and kept for 15 days and is thought to have 100% glycation (or browning). Samples 2 to 9 contained 50, 75, 100, 200, 300, 400, 500, and 600 µg/mL of myrrh. With an increase in myrrh concentration, the browning intensity (or potentially glycation) is revealed to be declining. Sample 10 contained BSA alone and it exhibited minimal browning intensity that might be due to some structural changes. The data are shown as means ± standard error of the means (n = 3, $p < 0.05$). The statistical differences are represented with an asterisk (*) for myrrh denoting significance at $p < 0.05$ in comparison with the reference sample.

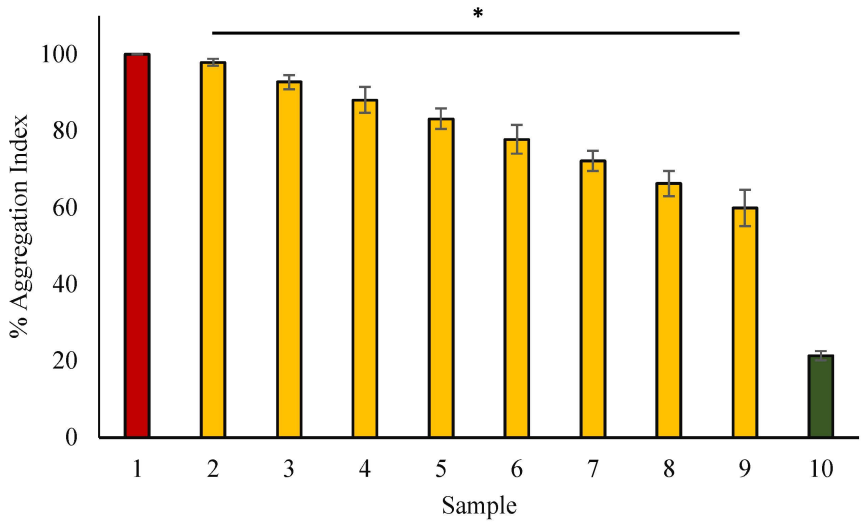

Figure 7. Decrease in aggregation index in presence of myrrh methanolic extract. Sample 1 is BSA treated with glucose for 15 days and is thought to have the highest aggregation index and hence the highest glycation aggregation index. Samples from 2 to 9 contained 50, 75, 100, 200, 300, 400, 500, and 600 μg/mL of myrrh extract. Sample 10 contained BSA incubated without glucose and myrrh and exhibited the minimal aggregation index. The data are shown as means ± standard error of the means (n = 3, $p < 0.05$). The statistical differences are represented with an asterisk (*) for myrrh denoting significance at $p < 0.05$ in comparison with the reference sample.

3.10. Congo Red Test

Figure 8 depicts the findings of the CR binding experiment. The study findings revealed that, at greater concentrations, myrrh extract considerably decreased cross-amyloid formations. In a concentration-dependent way, BSA samples containing glucose and myrrh extract revealed a considerable reduction in cross-amyloid aggregates when compared to BSA incubated with glucose alone ($p < 0.05$).

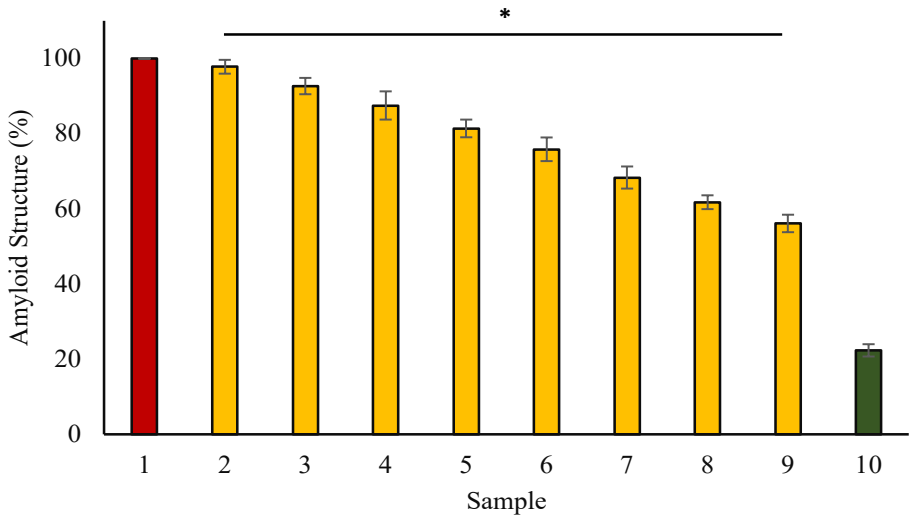

Figure 8. Reduction in cross-amyloid aggregates due to myrrh extract presence. Sample 1 refers to BSA treated with glucose for 15 days, and therefore is believed to have 100% structural changes. Samples 2–9 included 50, 75, 100, 200, 300, 400, 500, and 600 g/mL of myrrh, and cross-amyloid aggregates were found to decline as myrrh content increased. Sample 10 (green column) included BSA that had not been mixed with glucose or extract and had the fewest cross-amyloid aggregates. The data are shown as means ± standard error of the means (n = 3, $p < 0.05$). The statistical differences are represented with an asterisk (*) for myrrh denoting significance at $p < 0.05$ in comparison with the reference sample.

3.11. UV-Absorption Investigations

Our study shows that BSA treated with glucose (without extract) exhibits a considerably high absorption intensity at 280 nm compared to BSA incubated alone. The presence of myrrh extract in various glycated samples lead to a decrease in the hyperchromicity as compared to the glycated sample incubated without myrrh extract. As the content of extract increased, the hyperchromicity of the samples incubated with extract and glucose dropped dramatically (Figure 9) ($p < 0.05$).

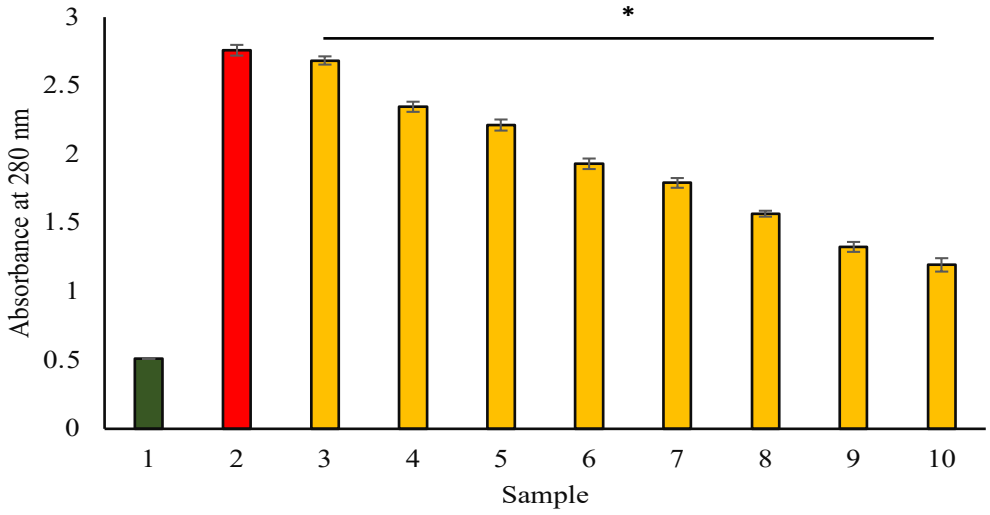

Figure 9. Absorbance at 280 nm vs. concentration (μg/mL)—Sample 1 (green pattern) shows native BSA that was incubated alone for 15 days, sample 2 (red pattern) represents BSA kept with glucose in the absence of myrrh extract for 15 days, samples 3 to 10 at X-axis indicate BSA kept for 15 days with glucose and myrrh extract's various concentrations (50, 75, 100, 200, 300, 400, 500, and 600 μg/mL) (yellow pattern). The data are shown as means ± standard error of the means (n = 3, $p < 0.05$). The statistical differences are represented with an asterisk (*) for myrrh denoting significance at $p < 0.05$ in comparison with the reference sample.

3.12. Effects of Extract on Fluorescent AGE Formation-Antiglycating Property

As the number of extracts increased, all of the samples incubated in the presence of extracts showed a continuous decrease in AGEs-specific fluorescence at 450 nm (Figure 10). The fluorescence intensity of BSA kept with glucose was at its maximum at 450 nm. These findings indicated that myrrh extract prevented the AGEs formation related to glycation, with the level of protection increased as the extract quantity was elevated ($p < 0.05$).

3.13. Effect of Myrrh Extract against Glycation Induced Fibrils Formation

According to our findings, increasing the extract concentration of myrrh extract in various glycated BSA samples is a major contributor to the steady decrease in ThT-specific fluorescence of these samples (Figure 11) ($p < 0.05$). As a consequence, our findings support myrrh extract's anti-amyloid action.

3.14. Investigation of Ligand-Receptor Interaction Using Molecular Docking

In this investigation, we explored the molecular interaction of significant antioxidants, catalase (PDB id: 1DGH), and superoxide dismutase (PDB id: 5YTU) with different active constituents of myrrh resin extract, including 2,3-Furandione, Curzerene, delta-Elemene, and Furanoeudesma-1,3-Diene. The binding energy and interacting amino acid residues of both antioxidants are presented in Table 2. As a conclusion, all of the concerned ligands are able to bind with both enzymes. The active residues mainly found in these interactions are Phe334, Val146, Tyr358, His75 and Leu144, Val14, Pro13, Gly12 in 1DGH, and 5YTU, respectively. The majority of residues are found in favorable regions, according to Ramachandran

plot analysis [35]. The results of different molecular docking investigations for exploring the interactions of functional residues present in 1DGH and 5YTU with ligands (bioactive molecules of myrrh) are shown in Figure 12.

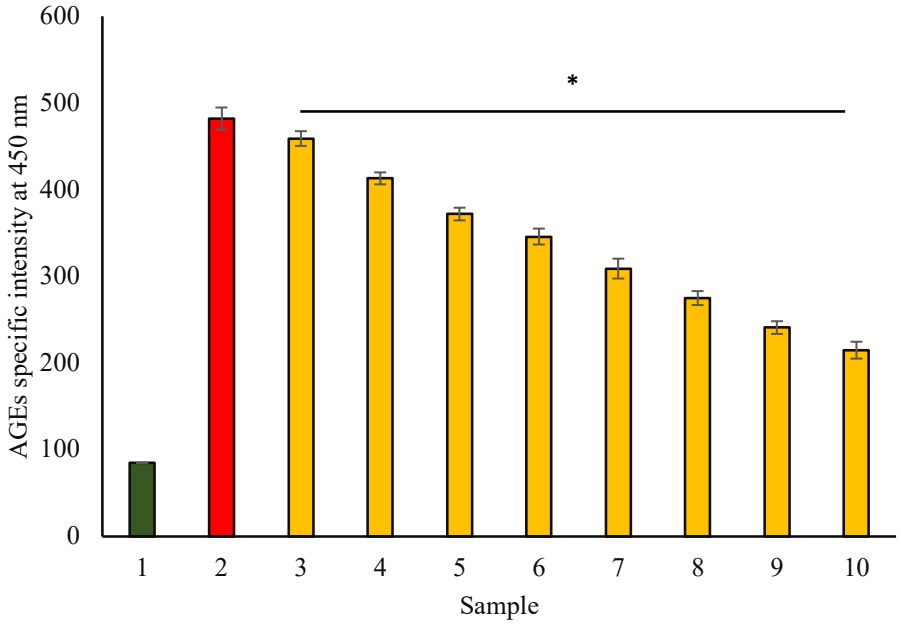

Figure 10. Fluorescence intensity at 450 nm vs. sample—Sample 1 (green pattern) shows native BSA that was incubated alone for 15 days, sample 2 (red pattern) represents BSA kept with glucose in the absence of myrrh extract for 15 days, samples 3 to 10 at X-axis indicate BSA kept for 15 days with glucose and myrrh extract's various concentrations (50, 75, 100, 200, 300, 400, 500, and 600 µg/mL) (yellow pattern). The data are shown as means ± standard error of the means (n = 3, $p < 0.05$). The statistical differences are represented with an asterisk (*) for myrrh denoting significance at $p < 0.05$ in comparison with the reference sample.

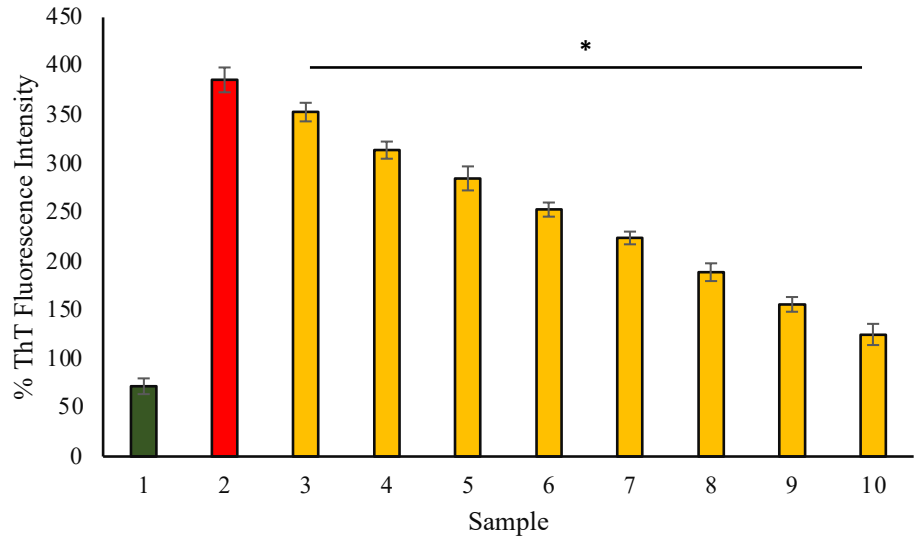

Figure 11. Fluorescence intensity at 480 nm vs. Sample—Sample 1 (green pattern) shows native BSA that was incubated alone for 15 days, sample 2 (red pattern) represents BSA kept with glucose in the absence of myrrh extract for 15 days, samples 3 to 10 at X-axis indicate BSA kept for 15 days with glucose and myrrh extract's various concentrations (50, 75, 100, 200, 300, 400, 500, and 600 µg/mL) (yellow pattern). The data are shown as means ± standard error of the means (n = 3, $p < 0.05$). The statistical differences are represented with an asterisk (*) for myrrh denoting significance at $p < 0.05$ in comparison with the reference sample.

Table 2. Specifications of docking investigations; the ligands, interacting functional residues (amino acids), and corresponding binding energy.

1. Catalase (1DGH)			
Ligands	**PubChem CID**	**Binding Energy (kcal/mol)**	**Interacting Amino Acids**
2,3-Furandione	13586830	−5.1	Phe334, Arg365, Arg72, Arg112
Curzerene	5316217	−7.7	Phe334, His75, Gly147, Ash148, Ala133, Arg354, Val146, Tyr358
delta-Elemene	12309449	−6.9	Val146, His75, Tyr358
Furanoeudesma-1,3-Diene	643237	−9.0	His75, Ala133, Val146, Val74, Tyr358, Arg72, Arg112, Phe334, Val73, Thr361, Ser114, Gly131, Phe132, Gly147, Asn148, Arg354
Positive Control: NADPH	5884	−10.2	Gly216, Arg354, Asp65, Tyr358, His75, Gly147, Ser114, Ala133, Arg72, Ile332, Arg112, Arg365, Phe161, Val146, Arg148, His218, Phe153, Leu299
2. Superoxide dismutase (5YTU)			
2,3-Furandione	13586830	−3.4	Asn65, His63
Curzerene	5316217	−2.5	Leu42, Asn86, Thr88
delta-Elemene	12309449	−4.2	Leu144, Glu121, His43, Thr39, Val14, Pro13, Gly12
Furanoeudesma-1,3-Diene	643237	−5.0	Asp11, Cys57, Leu144, Pro13, Val14, Gly12, Arg143, Gly10
Positive Control: Levisoprenaline	443372	−5.7	His63, Lys136, Lys70, Arg69, Asn65, Pro62

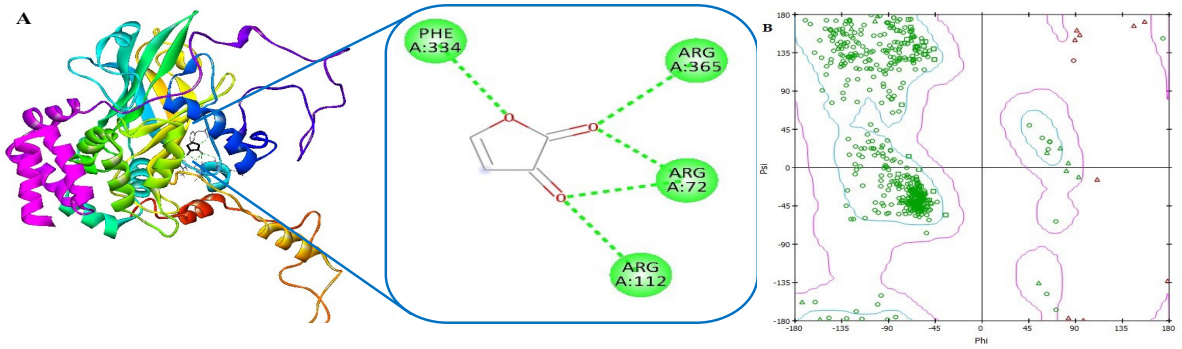

1. 1. Catalase (1DGH) and 2,3−Furandione

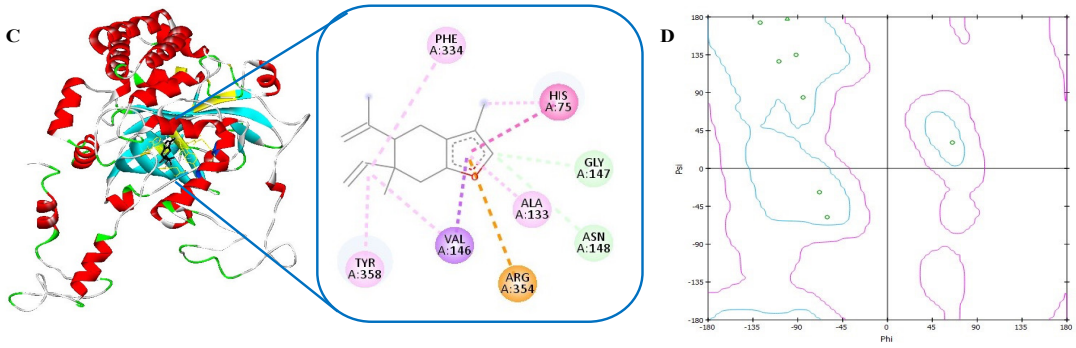

1. 2. Catalase (1DGH) and Curzerene

Figure 12. *Cont.*

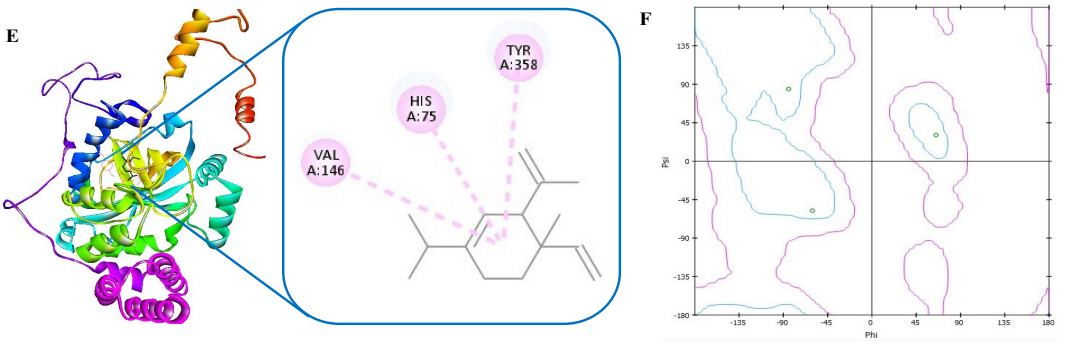

1. 3. Catalase (1DGH) and delta−Elemene

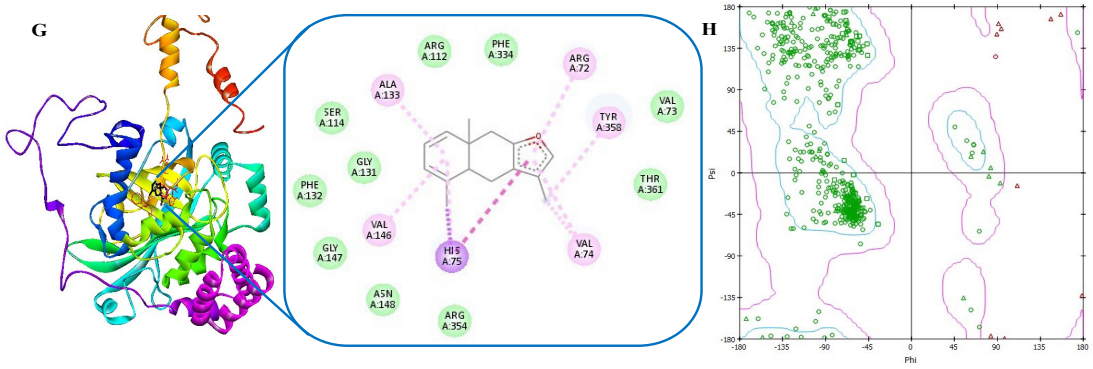

1.4. Catalase (1DGH) and Furanoeudesma−1,3−Diene

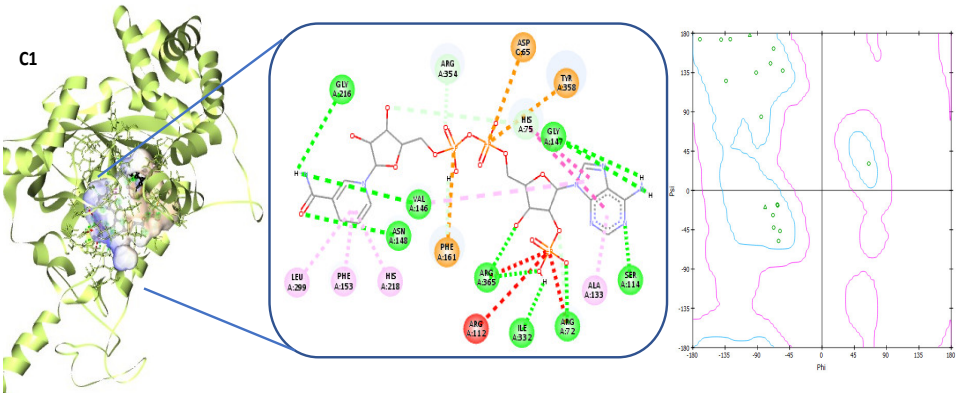

Positive Control 1: Catalase (1DGH) and NADPH

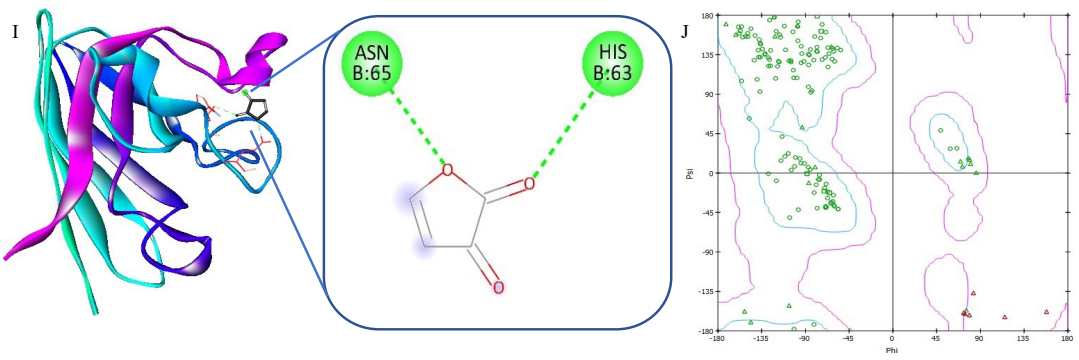

2.1. Superoxide dismutase (5YTU) and 2,3−Furandione

Figure 12. *Cont.*

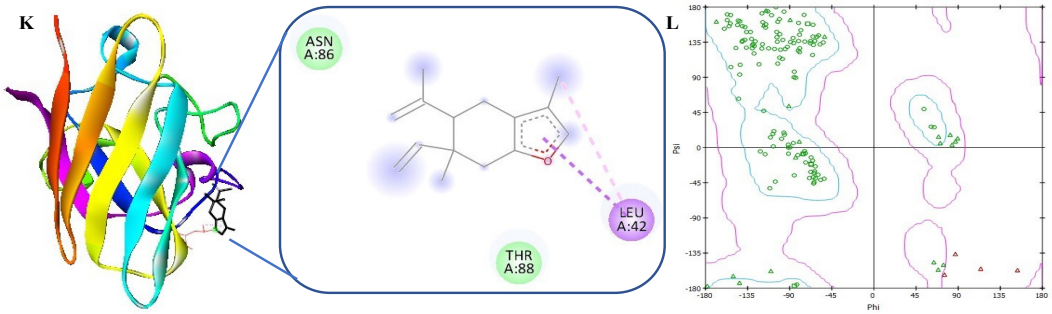

2.2. Superoxide dismutase (5YTU) and Curzerene

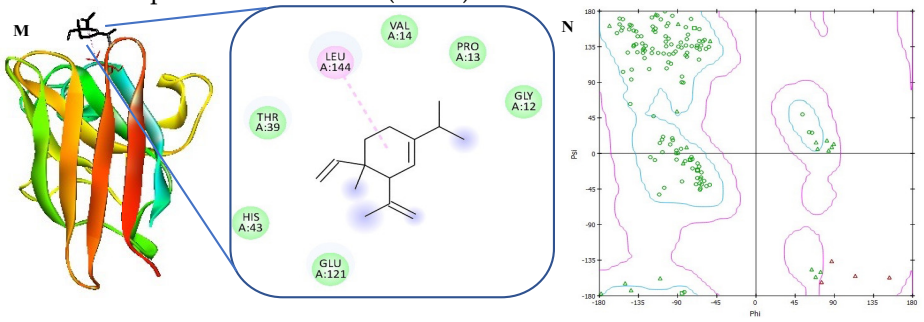

2.3. Superoxide dismutase (5YTU) and delta−Elemene

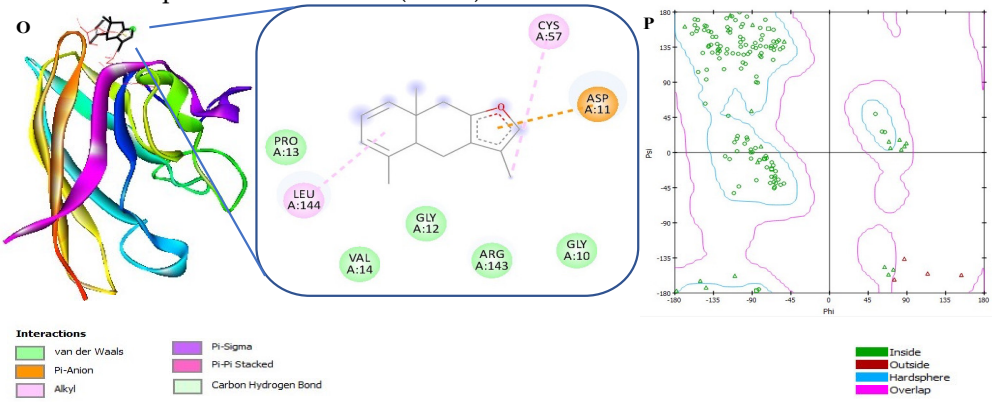

2.4. Superoxide dismutase (5YTU) and Furanoeudesma−1,3−Diene

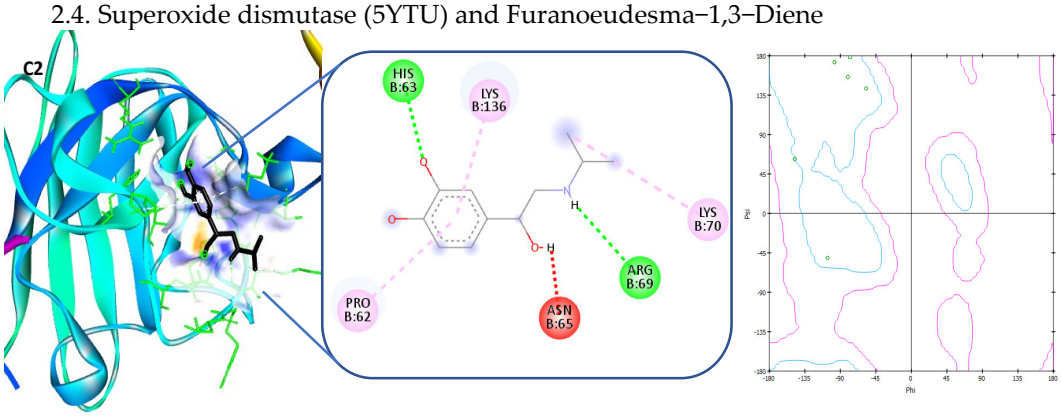

Positive Control 2: Superoxide dismutase (5YTU) and Levisoprenaline

Figure 12. The docking investigations highlighting the interactions of antioxidants including Catalase (1DGH) and Superoxide dismutase (5YTU) to bioactive components of myrrh resin extract with ligands (1) 2,3−Furandione (**A**,**I**); (2) Curzerene (**C**,**K**); (3) delta−Elemene (**E**,**M**); and (4) Furanoeudesma−1,3−Diene (**G**,**O**), respectively. With every protein-−ligand interaction, Ramachandran plots for corresponding interactions have been presented (**B**,**D**,**F**,**H**,**J**,**L**,**N**,**P**). The positive controls are shown in (**C1**,**C2**).

The study found that myrrh acts by directly causing the inactivation of free viral particles and interfering with the virion envelope structures, which are crucial for the virus to enter the host cells [36]. So, we studied the molecular interaction of SARS-CoV-2 spike protein S (6VXX) with active constituents of myrrh resin extract, 2,3-Furandione, Curzerene, delta-Elemene, and Furanoeudesma-1,3-Diene, to find the inhibitory action of these against the SARS-CoV-2 virus. The main functional residues found in interactions between two active constituents (Curzerene and Furanoeudesma-1,3-Diene) are Leu1024, Arg1039, Phe1042, and Thr1027, while the other two active constituents (2,3-Furandione and delta-Elemene) do not have common functional residues (Table 3) (Figure 13).

Table 3. Specifications of docking investigations; the ligands, interacting functional residues (amino acids) of receptor Spike protein S (6VXX), and corresponding binding energy.

3. Spike Protein S (6VXX)			
Ligands	**PubChem CID**	**Binding Energy (kcal/mol)**	**Interacting Amino Acids**
2,3-Furandione	13586830	−4.9	Ile870, Gly1059, His1058, Ala1056, Phe782, Val729, Thr778, Ser730, Pro863
Curzerene	5316217	−6.0	Leu1024, Arg1039, Phe1042, Thr1027, Asn1023
delta-Elemene	12309449	−5.8	Gln1010, Arg1014, Ile1013, Glu1017, Gln954, Ile1012, Arg1019, Ala1015, Glu773, Ile770, Gly769, Ala766, Arg765
Furanoeudesma-1,3-Diene	643237	−6.7	Ala1026, Glu780, Gln784, Ser1030, Glu1031, Thr1027, Asp1041, Val1040, Arg1039, Phe1042, Leu1024, Lys1028
Positive control: Acetylglucosamine	24139	−6.5	Arg1014, Arg765, Gln762

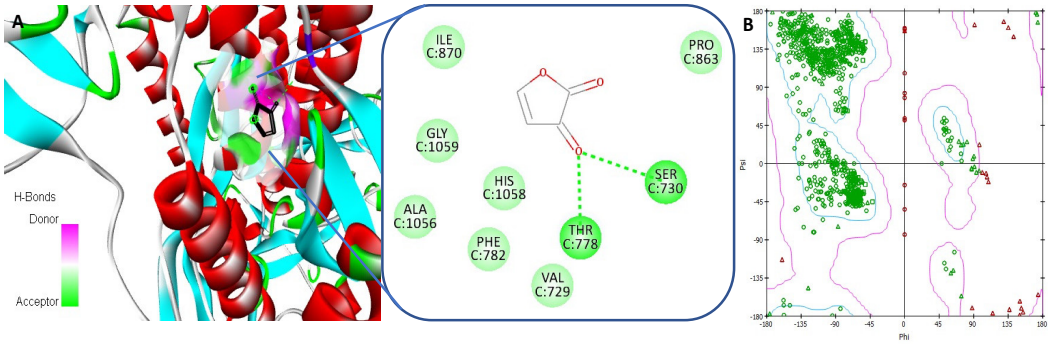

1.1. Receptor Spike protein S (6VXX) with 2,3−Furandione

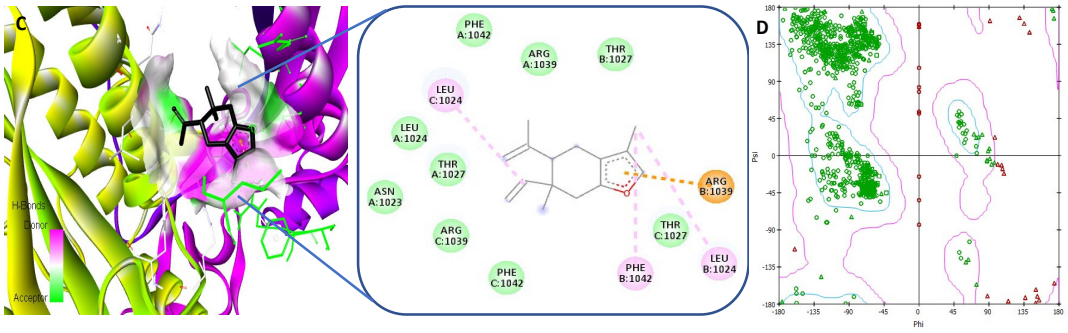

1.2. Receptor Spike protein S (6VXX) with Curzerene

Figure 13. *Cont.*

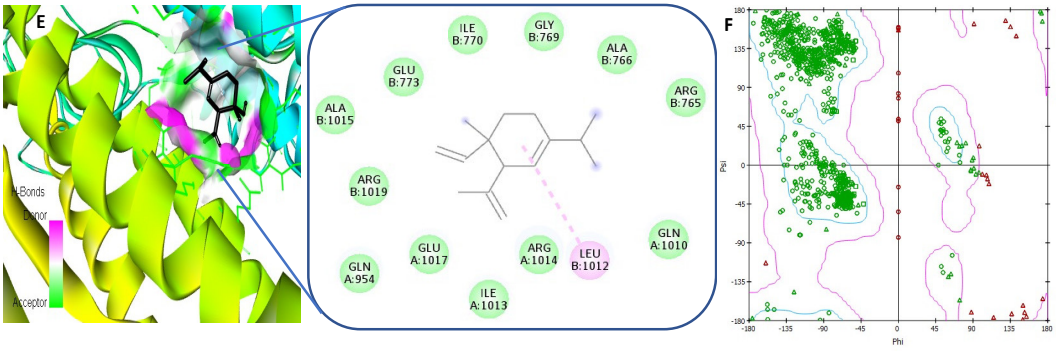

1.3. Receptor Spike protein S (6VXX) with delta−Elemene

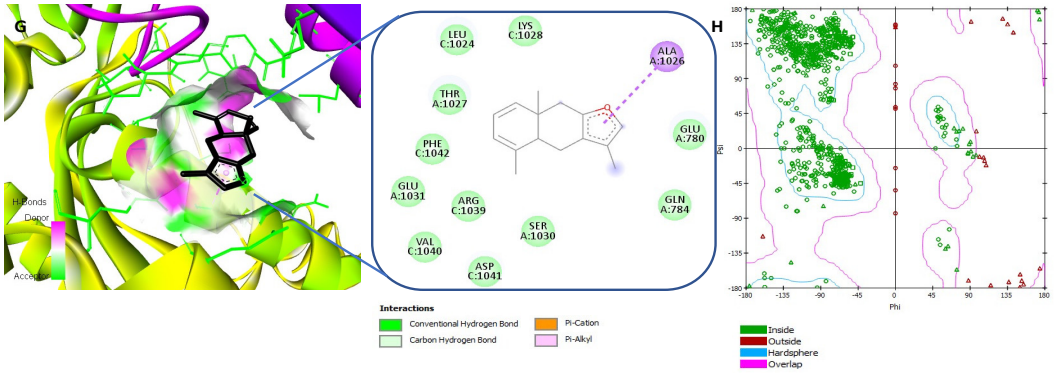

1.4. Receptor Spike protein S (6VXX) with Furanoeudesma−1,3−Diene

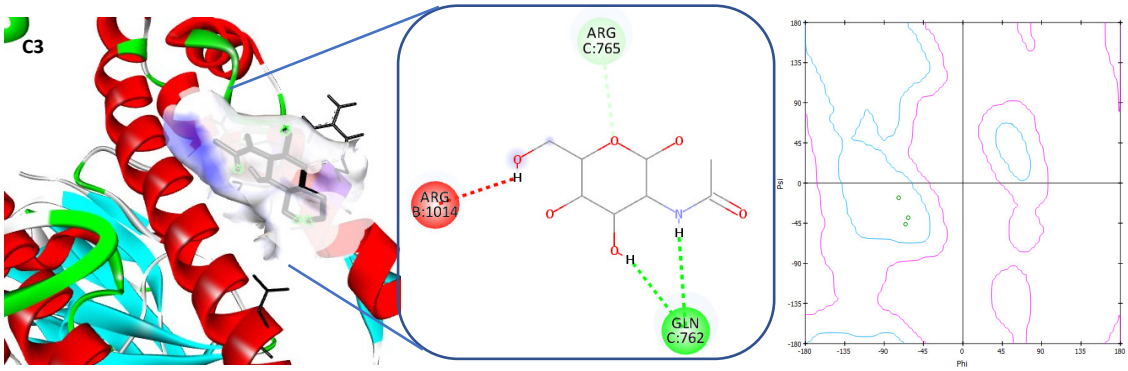

Positive Control 3: Receptor Spike protein S (6VXX) with Acetylglucosamine

Figure 13. The molecular docking studies of receptor Spike protein S (6VXX) with active constituents of myrrh resin extract with ligands (1) 2,3−Furandione (**A**); (2) Curzerene (**C**); (3) delta−Elemene (**E**); and (4) Furanoeudesma−1,3−Diene (**G**), respectively. The Ramachandran plots of corresponding interactions have been presented to every protein–ligand interaction (**B**,**D**,**F**,**H**). The positive control is shown in (**C3**).

4. Discussion

Guggul, Opopanax, Bdellium, Bisabol, and Balsam are popular names for myrrh, which has been used as a medicine since ancient times. It was used as medicine and perfume for thousands of years in the ancient world. It has been utilized in various ways, including mixing it with warm water or ingesting it in the form of resin. Saudi Arabia, Ethiopia, Yemen, Somalia, Oman, and Eritrea are among the countries where myrrh is found. Myrrh is commonly used as a traditional remedy for coughs, cancer, ulcers,

colds, dyspepsia, gastrointestinal tract (GI) problems, arthritis, wound healing, and lung congestion, which are all treated with myrrh gum. The effect of myrrh resin in therapeutic interventions was explored in this research using *in silico* and *in vitro* analyses.

Furanoeudesma-1,3-diene, curzerene, and elemene are the three main components of myrrh, according to a recent study by Madia and colleagues (2021) [37]. However, the primary ingredient in oils and extracts was furandione [38]. In the current study, all ingredients were put to the test, including furanoeudesma-1,3-diene, curzerene, delta−elemene, and furandione.

Numerous illnesses, including diabetes and its consequences, are linked to oxidative stress, systemic hyper-inflammatory responses, glycation of biomolecules, production of AGEs, and permeabilization of the lysosomal membrane. The current study showed that myrrh extract offered maximum inhibition against heat-induced denaturation of bovine serum albumin (53.47%), and exhibited maximum anti-proteinase action (43.517%), and significant inhibition of egg albumin denaturation (44.95%) at a dose of 600 µg/mL concentration as compared to controls. Additionally, myrrh extract at a dose of 600 µg/mL had been found to decrease browning intensity (59.38%), inhibit the percent aggregation index by 59.88%, as well as reduce the percentage amyloid structure (56.13%). Polyphenolic compounds, especially flavonoids, have been reported to have positive health effects due to their antioxidant, anti-inflammatory, antiglycation activity, and the AGEs formation inhibition activities of several plant extracts [5,39]. Our research found that myrrh resin has considerable antioxidant activity, which might explain its medicinal potential against oxidative stress, protein denaturation, and AGE production. ROS have a role in gene expression, signal transduction, and receptor activation, among other things [9].

Fruits and vegetables contain polyphenols, which have health-promoting and sensorial characteristics. Polyphenols also have a role in the structure-dependent stability of foods during processing and storage [40]. Antioxidant-rich compounds can prevent oxidative damage by protecting cell organelles, organs, and tissues from ROS and oxidative stress [20]. In this perspective, screening of plant-based natural products as a source of therapeutically essential antioxidant molecules with substantial medicinal activity is receiving a lot of interest [11].

Glycation results in structural alterations in biomolecules such as proteins. The structural flaw could result in aggregates. Various diseases and their consequences are linked to the production of protein aggregates. In order to develop a strategy for treating and controlling illnesses linked to the aggregate formation or structural modification brought on by glycation, it is imperative to investigate the protective efficacy of natural products against glycation-induced protein aggregation formation [41].

Myrrh extract included large amounts of polyphenolic chemicals and flavonoids. The capacity of the extract to scavenge free radicals using the DPPH method revealed that myrrh suppressed free radicals in a concentration-dependent way. Higher levels of polyphenolic chemicals may be responsible for the considerable reduction of free radicals [42]. Myrrh extracts have a high level of H_2O_2 scavenging action. It is generally known that the breakdown of H_2O_2 produces hydroxyl free radicals in the blood. Hydroxyl radicals are produced by the breakdown of H_2O_2 and the activation of neutrophils, and are thought to play a key role in the oxidative stress linked to acute lung injury [43]. Antioxidants have been demonstrated to reduce the activation of NF-kB by H_2O_2 as well as all other inducers [44]. DNA damage and the activation of oncogenes such as K-ras and C-Raf-1 have both been linked to hydroxyl free radicals [45].

Our findings show that myrrh extracts can prevent heat-mediated denaturation of albumin and egg albumin, which have been linked to rheumatoid arthritis. The ability to inhibit albumin denaturation was evaluated to establish the basis of myrrh extract's anti-inflammatory activity. As a result, it may be stated that myrrh extract has significant anti-inflammatory properties. Furthermore, protein denaturation results in the production of autoantibodies [46].

The presence of medicinally active flavonoids in myrrh extract may account for this capacity [47]. Furthermore, anti-proteinase activity is thought to protect against tissue damage caused by proteinase [39,48]. Additionally, the deposition of auto-antigens in the synovial joints is likely to cause joint inflammation. The activation of matrix metalloproteins by ROS is considered to be involved in severe tissue destruction, such as that found in different arthritic responses of the body [21].

Inhibitors of glycation and AGE production may thus be effective in the prevention and treatment of diabetic complications [2], as well as cancer [49]. In the current study, myrrh extract substantially decreased browning intensity, AGE production, and cross-amyloid formations in a concentration-dependent way, compared to all other research on glycation and AGE formation. It has been previously suggested that antioxidant activity, polyphenolic content, and AGEs formation inhibition are linked with each other [39]. As a result, the quantity of polyphenolic chemicals with high antioxidant activity may be responsible for myrrh extract's ability to suppress the production of AGEs.

Flavonoids and other polyphenolic substances have been shown to protect against the development of cancer [50]. We conducted a molecular docking investigation to confirm the molecular defenses of myrrh phytoconstituents against oxidative stress and conformational alterations of anti-oxidant enzymes as well as to link numerous potential compounds of myrrh to special chemical features. This further confirms our hypothesis that myrrh extract may be capable of protecting these enzymes from denaturation caused by glycation, as well as defending from various oxidative stress-mediated health ailments. Furthermore, a molecular docking investigation was conducted between the SARS-CoV-2 Spike protein S and myrrh extract constituents to identify SARS-CoV-2 virus inhibitors, and to validate the concept that Myrrh extract can block SARS-CoV-2 virus' access into human cells due to its ability to bind viral proteins. It is already discussed that spike (S) glycoproteins of the SARS-CoV-2 virus facilitate this virus' entrance into the cell via interaction with ACE2 [31,51]. From these docking studies, it was seen that the interaction of these myrrh extract constituents and Spike protein S could possibly suggest the inhibitory action of myrrh extract against the SARS-CoV-2 virus.

Through in vitro tests, our research supports the therapeutic benefits of myrrh against the pathophysiology of different health ailments. Myrrh extract may be used to reduce oxidative stress linked with glycation-induced denaturation of these antioxidants in diabetic patients. Additionally, the ability of myrrh ligands to bind with spike proteins can be used in the development of anti-spike and antiviral drugs for SARS-CoV-2 because of the ability of its constituents to interact with spike proteins, as seen in our docking studies. As a result, it is possible to propose the consumption of myrrh resin from locally farmed myrrh for the prevention of various diseases, and their therapeutics. However, identifying and validating the various mechanisms of myrrh components in modifying these diseases through in vivo experiments using a human model is very critical in this context.

5. Conclusions

Myrrh resin is considered to have a variety of beneficial substances. The mechanism of myrrh responsible for the prevention of various diseases has yet to be established, however, it is most likely connected to its particular structures. Myrrh extract demonstrated strong antioxidant activity, inhibited heat-mediated denaturation of protein, protected BSA from browning induced by glucose, as well as prevented the formation of AGEs and cross-amyloid structures. Contrarily, clinical trials are required to support its efficacy in in vivo settings. The in silico molecular docking analysis proves the binding interactions between antioxidant enzymes, catalase, superoxide dismutase, and the SARS-CoV-2 spike protein (S) with active constituents of myrrh. The different phytoconstituents used in this study may be used to treat COVID-19 and may pave the way for the future development of more effective natural antivirals against COVID-19 if they are confirmed on experimental models by in vivo investigations. Thus, our data projects it to be the possible therapeutic target of various diseases associated with diabetes and oxidative stress. Furthermore, these in

silico results need to be validated by in vitro tests and molecular simulations. It is very necessary to conduct quantitative or semi-quantitative values estimations of phytochemical screening for understanding the therapeutic mechanism of myrrh. Before choosing myrrh as a potential therapeutic lead, the limitations such as interactions of the compounds with all biomolecules, cells, and tissues (i.e., systems biology) need to be adjusted.

Author Contributions: Conceptualization, S.A. and A.H.R.; Investigation, M.A.A.; Methodology, S.A., A.H.R., R.R., A.A., M.A.A. and S.A.A.; Supervision, M.A.A., A.A. and A.A.K.; writing—original draft, S.A., A.H.R. and R.R. writing—review & editing, M.A.A., A.Y.B., A.A., A.A.K., S.A.A. and A.H.R. All authors have read and agreed to the published version of the manuscript.

Funding: This research work was funded by the Deputyship for Research & Innovation, Ministry of Education, Saudi Arabia, through project number QU-IF-2-2-1-26522.

Institutional Review Board Statement: Not applicable.

Informed Consent Statement: Not applicable.

Data Availability Statement: The data used to support the findings of this study are included within the article.

Acknowledgments: The authors extend their appreciation to the Deputyship for Research & Innovation, Ministry of Education, Saudi Arabia for funding this research work through the project number (QU-IF-2-2-1-26522). The authors also thank to Qassim University for technical support.

Conflicts of Interest: The authors declare no conflict of interest for this work.

References

1. Yalcin Kehribar, D.; Cihangiroglu, M.; Sehmen, E.; Avci, B.; Capraz, A.; Yildirim Bilgin, A.; Gunaydin, C.; Ozgen, M. The receptor for advanced glycation end product (RAGE) pathway in COVID-19. *Biomark. Biochem. Indic. Expo. Response Susceptibility Chem.* **2021**, *26*, 114–118. [CrossRef] [PubMed]
2. Younus, H.; Anwar, S. Prevention of non-enzymatic glycosylation (glycation): Implication in the treatment of diabetic complication. *Int. J. Health Sci.* **2016**, *10*, 261–277. [CrossRef]
3. Sartore, G.; Ragazzi, E.; Faccin, L.; Lapolla, A. A role of glycation and methylation for SARS-CoV-2 infection in diabetes? *Med. Hypotheses* **2020**, *144*, 110247. [CrossRef] [PubMed]
4. Vargas-Rodriguez, J.R.; Garza-Veloz, I.; Flores-Morales, V.; Badillo-Almaraz, J.I.; Rocha-Pizaña, M.R.; Valdés-Aguayo, J.J.; Martinez-Fierro, M.L. Hyperglycemia and Angiotensin-Converting Enzyme 2 in Pulmonary Function in the Context of SARS-CoV-2 Infection. *Front. Med.* **2022**, *8*, 758414. [CrossRef] [PubMed]
5. Anwar, S.; Raut, R.; Alsahli, M.A.; Almatroudi, A.; Alfheeaid, H.; Alzahrani, F.M.; Khan, A.A.; Allemailem, K.S.; Almatroodi, S.A.; Rahmani, A.H. Role of Ajwa Date Fruit Pulp and Seed in the Management of Diseases through In Vitro and In Silico Analysis. *Biology* **2022**, *11*, 78. [CrossRef]
6. Anwar, S.; Almatroudi, A.; Allemailem, K.S.; Jacob Joseph, R.; Khan, A.A.; Rahmani, A.H. Protective Effects of Ginger Extract against Glycation and Oxidative Stress-Induced Health Complications: An In Vitro Study. *Processes* **2020**, *8*, 468. [CrossRef]
7. Anwar, S.; Khan, S.; Almatroudi, A.; Khan, A.A.; Alsahli, M.A.; Almatroodi, S.A.; Rahmani, A.H. A review on mechanism of inhibition of advanced glycation end products formation by plant derived polyphenolic compounds. *Mol. Biol. Rep.* **2021**, *48*, 787–805. [CrossRef]
8. Ansari, N.A.; Rasheed, Z. Non-enzymatic glycation of proteins: From diabetes to cancer. *Biomeditsinskaia Khimiia* **2010**, *56*, 168–178. [CrossRef]
9. Alsahli, M.A.; Anwar, S.; Alzahrani, F.M.; Almatroudi, A.; Alfheeaid, H.; Khan, A.A.; Allemailem, K.S.; Almatroodi, S.A.; Rahmani, A.H. Health Promoting Effect of Phyllanthus emblica and Azadiractha indica against Advanced Glycation End Products Formation. *Appl. Sci.* **2021**, *11*, 8819. [CrossRef]
10. Singh, V.P.; Bali, A.; Singh, N.; Jaggi, A.S. Advanced glycation end products and diabetic complications. *Korean J. Physiol. Pharmacol. Off. J. Korean Physiol. Soc. Korean Soc. Pharmacol.* **2014**, *18*, 1–14. [CrossRef]
11. Meenatchi, P.; Purushothaman, A.; Maneemegalai, S. Antioxidant, antiglycation and insulinotrophic properties of *Coccinia grandis* (L.) in vitro: Possible role in prevention of diabetic complications. *J. Tradit. Complement. Med.* **2016**, *7*, 54–64. [CrossRef] [PubMed]
12. Chen, Y.; Zhou, C.; Ge, Z.; Liu, Y.; Liu, Y.; Feng, W.; Li, S.; Chen, G.; Wei, T. Composition and potential anticancer activities of essential oils obtained from myrrh and frankincense. *Oncol. Lett.* **2013**, *6*, 1140–1146. [CrossRef] [PubMed]
13. Eid, R.A.A. Efficacy of Commiphora myrrh mouthwash on early wound healing after tooth extraction: A randomized controlled trial. *Saudi Dent. J.* **2021**, *33*, 44–54. [CrossRef]
14. Sotoudeh, R.; Hadjzadeh, M.-A.-R.; Gholamnezhad, Z.; Aghaei, A. The anti-diabetic and antioxidant effects of a combination of Commiphora mukul, Commiphora myrrha and Terminalia chebula in diabetic rats. *Avicenna J. Phytomed.* **2019**, *9*, 454–464. [PubMed]

15. Shalaby, M.A.; Hammouda, A.A.-E. Analgesic, anti-inflammatory and anti-hyperlipidemic activities of Commiphora molmol extract (Myrrh). *J. Intercult. Ethnopharmacol.* **2014**, *3*, 56–62. [CrossRef] [PubMed]
16. Nohr, L.A.; Rasmussen, L.B.; Straand, J. Resin from the mukul myrrh tree, guggul, can it be used for treating hypercholesterolemia? A randomized, controlled study. *Complement. Ther. Med.* **2009**, *17*, 16–22. [CrossRef] [PubMed]
17. Almatroodi, S.A.; Almatroudi, A.; Anwar, S.; Yousif Babiker, A.; Khan, A.A.; Alsahli, M.A.; Rahmani, A.H. Antioxidant, anti-inflammatory and hepatoprotective effects of olive fruit pulp extract: In vivo and in vitro study. *J. Taibah Univ. Sci.* **2020**, *14*, 1660–1670. [CrossRef]
18. Anwar, S.; Almatroodi, S.A.; Almatroudi, A.; Allemailem, K.S.; Joseph, R.J.; Khan, A.A.; Alrumaihi, F.; Alsahli, M.A.; Husain Rahmani, A. Biosynthesis of silver nanoparticles using Tamarix articulata leaf extract: An effective approach for attenuation of oxidative stress mediated diseases. *Int. J. Food Prop.* **2021**, *24*, 677–701. [CrossRef]
19. Chatterjee, P.; Chandra, S.; Dey, P.; Bhattacharya, S. Evaluation of anti-inflammatory effects of green tea and black tea: A comparative in vitro study. *J. Adv. Pharm. Technol. Res.* **2012**, *3*, 136–138. [CrossRef]
20. Almatroodi, S.A.; Anwar, S.; Almatroudi, A.; Khan, A.A.; Alrumaihi, F.; Alsahli, M.A.; Rahmani, A.H. Hepatoprotective Effects of Garlic Extract against Carbon Tetrachloride (CCl4)-Induced Liver Injury via Modulation of Antioxidant, Anti-Inflammatory Activities and Hepatocyte Architecture. *Appl. Sci.* **2020**, *10*, 6200. [CrossRef]
21. Sakat, S.; Juvekar, A.; Gambhire, M. In vitro antioxidant and anti inflammatory activity of methanol extract of *Oxalis corniculata* Linn. *Chemistry* **2010**, *2*, 146–155. [CrossRef]
22. Brownlee, M.; Vlassara, H.; Kooney, A.; Ulrich, P.; Cerami, A. Aminoguanidine prevents diabetes-induced arterial wall protein cross-linking. *Science* **1986**, *232*, 1629–1632. [CrossRef]
23. Schrodel, A.; de Marco, A. Characterization of the aggregates formed during recombinant protein expression in bacteria. *BMC Biochem.* **2005**, *6*, 10. [CrossRef]
24. Anwar, S.; Khan, M.A.; Sadaf, A.; Younus, H. A structural study on the protection of glycation of superoxide dismutase by thymoquinone. *Int. J. Biol. Macromol.* **2014**, *69*, 476–481. [CrossRef]
25. Anwar, S.; Younus, H. Anti-glycating potential of ellagic acid against glucose and methylglyoxal-induced glycation of superoxide dismutase. *J. Proteins Proteom.* **2017**, *8*, 1–12.
26. Anwar, S.; Younus, H. Inhibitory effect of alliin from Allium sativum on the glycation of superoxide dismutase. *Int. J. Biol. Macromol.* **2017**, *103*, 182–193. [CrossRef]
27. Dar, A.M.; Mir, S. Molecular Docking: Approaches, Types, Applications and Basic Challenges. *J. Anal. Bioanal. Tech.* **2017**, *8*, 356. [CrossRef]
28. Schröter, D.; Höhn, A. Role of Advanced Glycation End Products in Carcinogenesis and their Therapeutic Implications. *Curr. Pharm. Des.* **2018**, *24*, 5245–5251. [CrossRef]
29. Putnam, C.D.; Arvai, A.S.; Bourne, Y.; Tainer, J.A. Active and inhibited human catalase structures: Ligand and NADPH binding and catalytic mechanism11Edited by R. Huber. *J. Mol. Biol.* **2000**, *296*, 295–309. [CrossRef] [PubMed]
30. Manjula, R.; Wright, G.S.A.; Strange, R.W.; Padmanabhan, B. Assessment of ligand binding at a site relevant to SOD1 oxidation and aggregation. *FEBS Lett.* **2018**, *592*, 1725–1737. [CrossRef]
31. Walls, A.C.; Park, Y.-J.; Tortorici, M.A.; Wall, A.; McGuire, A.T.; Veesler, D. Structure, Function, and Antigenicity of the SARS-CoV-2 Spike Glycoprotein. *Cell* **2020**, *181*, 281–292.e6. [CrossRef] [PubMed]
32. Ahamad, S.R.; Al-Ghadeer, A.R.; Ali, R.; Qamar, W.; Aljarboa, S. Analysis of inorganic and organic constituents of myrrh resin by GC–MS and ICP-MS: An emphasis on medicinal assets. *Saudi Pharm. J.* **2017**, *25*, 788–794. [CrossRef]
33. Sunghwan, K.; Chen, j.; Cheng, T.; Gindulyte, A.; Jia, H. PubChem in 2021: New data content and improved web interfaces. *Nucleic Acids Res.* **2021**, *49*, D1388–D1395. [CrossRef]
34. Morris, G.M.; Huey, R.; Lindstrom, W.; Sanner, M.F.; Belew, R.K.; Goodsell, D.S.; Olson, A.J. AutoDock4 and AutoDockTools4: Automated docking with selective receptor flexibility. *J. Comput. Chem.* **2009**, *30*, 2785–2791. [CrossRef] [PubMed]
35. Ramachandran, G.N.; Ramakrishnan, C.; Sasisekharan, V. Stereochemistry of polypeptide chain configurations. *J. Mol. Biol.* **1963**, *7*, 95–99. [CrossRef]
36. Brochot, A.; Guilbot, A.; Haddioui, L.; Roques, C. Antibacterial, antifungal, and antiviral effects of three essential oil blends. *MicrobiologyOpen* **2017**, *6*, e00459. [CrossRef] [PubMed]
37. Madia, V.N.; De Angelis, M.; De Vita, D.; Messore, A.; De Leo, A.; Ialongo, D.; Tudino, V.; Saccoliti, F.; De Chiara, G.; Garzoli, S.; et al. Investigation of Commiphora myrrha (Nees) Engl. Oil and Its Main Components for Antiviral Activity. *Pharmaceuticals* **2021**, *14*, 243. [CrossRef]
38. Messina, F.; Gigliarelli, G.; Palmier, A.; Marcotullio, M.C. Furanodienone: An Emerging Bioactive Furanosesquiterpenoid. *Curr. Org. Chem.* **2017**, *21*, 305–310. [CrossRef]
39. Anwar, S.; Almatroudi, A.; Alsahli, M.A.; Khan, M.A.; Khan, A.A.; Rahmani, A.H. Natural Products: Implication in Cancer Prevention and Treatment through Modulating Various Biological Activities. *Anticancer Agents Med. Chem.* **2020**, *20*, 2025–2040. [CrossRef]
40. Hanuka Katz, I.; Eran Nagar, E.; Okun, Z.; Shpigelman, A. The Link between Polyphenol Structure, Antioxidant Capacity and Shelf-Life Stability in the Presence of Fructose and Ascorbic Acid. *Molecules* **2020**, *25*, 225. [CrossRef]
41. Sirangelo, I.; Iannuzzi, C. Understanding the Role of Protein Glycation in the Amyloid Aggregation Process. *Int. J. Mol. Sci.* **2021**, *22*, 6609. [CrossRef]
42. Chu, Y.-F.; Sun, J.; Wu, X.; Liu, R.H. Antioxidant and Antiproliferative Activities of Common Vegetables. *J. Agric. Food Chem.* **2002**, *50*, 6910–6916. [CrossRef]

43. Derouiche, S. Oxidative Stress Associated with SARS-Cov-2 (COVID-19) Increases the Severity of the Lung Disease—A Systematic Review. *J. Infect. Dis. Epidemiol.* **2020**, 6. [CrossRef]
44. Schreck, R.; Albermann, K.; Baeuerle, P.A. Nuclear Factor Kb: An Oxidative Stress-Responsive Transcription Factor of Eukaryotic Cells (A Review). *Free. Radic. Res. Commun.* **1992**, *17*, 221–237. [CrossRef]
45. Pourahmad, J.; Salimi, A.; Seydi, E. Role of Oxygen Free Radicals in Cancer Development and Treatment. In *Free Radicals and Diseases*; Ahmad, R., Ed.; IntechOpen: Vienna, Austria, 2016. [CrossRef]
46. Williams, L.A.D.; O'Connar, A.; Latore, L.; Dennis, O.; Ringer, S.; Whittaker, J.A.; Conrad, J.; Vogler, B.; Rosner, H.; Kraus, W. The in vitro anti-denaturation effects induced by natural products and non-steroidal compounds in heat treated (immunogenic) bovine serum albumin is proposed as a screening assay for the detection of anti-inflammatory compounds, without the use of animals, in the early stages of the drug discovery process. *West Indian Med. J.* **2008**, *57*, 327–331.
47. Havsteen, B.H. The biochemistry and medical significance of the flavonoids. *Pharmacol. Ther.* **2002**, *96*, 67–202. [CrossRef]
48. Brown, J.H.; Mackey, H.K. Inhibition of Heat-Induced Denaturation of Serum Proteins by Mixtures of Nonsteroidal Anti-Inflammatory Agents and Amino Acids. *Proc. Soc. Exp. Biol. Med.* **1968**, *128*, 225–228. [CrossRef]
49. Turner, D.P. Advanced glycation end-products: A biological consequence of lifestyle contributing to cancer disparity. *Cancer Res.* **2015**, *75*, 1925–1929. [CrossRef]
50. Liu, R.H. Potential Synergy of Phytochemicals in Cancer Prevention: Mechanism of Action. *J. Nutr.* **2004**, *134*, 3479S–3485S. [CrossRef]
51. Shang, J.; Wan, Y.; Luo, C.; Ye, G.; Geng, Q.; Auerbach, A.; Li, F. Cell entry mechanisms of SARS-CoV-2. *Proc. Natl. Acad. Sci. USA* **2020**, *117*, 11727–11734. [CrossRef]